Original Paper

Received: 19 May 2011 / Revised: 22 July 2011 / Accept: 24 July 2011

Studying pigments on painted plaster in Minoan, Roman and Early Byzantine Crete. A multi-analytical technique approach

P. Westlake[1], P. Siozos[2], A. Philippidis[2], C. Apostolaki[4], B. Derham[5], A. Terlixi[6], V. Perdikatsis[4], R. Jones[5], D. Anglos[2,3,*]

[1] British School at Athens, Knossos Villa Ariadne Taverna, 714 09 Knossos, Crete, Greece

[2] Institute of Electronic Structure and Laser, Foundation for Research and Technology-Hellas (IESL-FORTH), P.O. Box 1385, 711 10 Heraklion, Crete, Greece

[3] Department of Chemistry, University of Crete, P.O.Box 2208, 710 03 Heraklion, Crete, Greece

[4] Department of Mineral Resources Engineering, Technical University of Crete, 731 00 Chania, Crete, Greece

[5] Department of Archaeology, University of Glasgow, Glasgow G12 8QQ, UK

[6] Department of Conservation of Works of Art, National Gallery of Athens, 1 Michalacopoulou St., 116 01 Athens, Greece

**Author to whom correspondence should be addressed*: anglos@iesl.forth.gr

Footnote: Published in the special issue *Analytical Techniques in Art, Archaeology and Conservation Science* with guest editor Oliver Hahn.

Note to vendor, for copy editing: Please do not change the footnote.

Abstract

Wall paintings spanning two millennia of Cretan painting history and technology were analysed in an effort to determine similarities and evolutions of painting materials and technology. A multi-technique approach was employed that combined the use of a) laser-induced breakdown spectroscopy (LIBS) and Raman microspectroscopy, based on mobile instrumentation, appropriate for rapid, routine-level object characterization, and b) non-destructive x-ray diffractometry (XRD), performed directly on the wall painting fragment, that provides detailed information on the minerals constituting the paint. Elemental analysis data obtained through LIBS were compared to molecular and crystal structure information featured by Raman spectroscopy and XRD. Cross-sections from selected samples were also investigated by means of optical microscopy and scanning electron microscopy coupled to micro-probe analysis and x-ray mapping that enabled identification of several mineral components of the paint confirming the results of the XRD analysis. In parallel, replica wall paintings, created with known pigments and binding media, for reference purposes; were examined with optical microscopy and stain tested for organic materials. The overall study shows that the LIBS and Raman techniques offer key advantages, such as instrument mobility and speed of data collection and interpretation that are particularly important when dealing with on site investigations. Thus they are capable of providing important compositional information in an effective manner that enables quick surveying of wall paintings and permit targeted sample selection for further analysis by advanced laboratory techniques.

Keywords: archaeological pigments, wall paintings, analysis, LIBS, Raman, XRD, SEM-EDX

1. Introduction

Materials analysis has long been recognised as an essential component of archaeological research. It yields critical compositional information that may lead to object characterization, revealing ingredients and technologies used by craftsmen, or even providing insight to technology exchanges, communication and trade. [1,2,3] Furthermore, in the context of object conservation, it allows informed decisions necessary for proper conservation/restoration of objects to be made. [4] Indeed, several advanced materials analysis techniques are being used in archaeological research and conservation science but, to-date, their use is primarily confined in the premises of specialized research laboratories or large scientific facilities. [5,6] On the other hand, there is growing motivation for the use of modern analytical methods on site and in real time, for example, during excavation or survey campaigns and in subsequent conservation work. [7,8] Evidently the need for compact analytical instruments and versatile, robust, non-destructive methodologies that would avoid sampling and enable analytical studies to be performed rapidly, routinely and non-destructively, in the context of the museum or conservation laboratory, is an important challenge. Furthermore it is highly desirable to have techniques and instruments available that can be operated by skilled archaeologists and conservation staff *in situ,* not requiring the presence of specialised research scientists or technicians. This would enable more effective conservation procedures and excavation decisions to be undertaken rapidly and decisively for the benefit of the long-term preservation of cultural heritage. It would also increase the availability of suitable collections for more focused and time-consuming analysis in the post-excavation stage by enabling an effective sample 'screening process' to take place.

The present multi-analytical technique study is part of a broader project that aims to explore the wall painting pigments used on the island of Crete from the Bronze Age to the Roman and Byzantine periods. A fairly large body of work exists on the analysis of pigments used in Bronze Age wall paintings from Crete [9,10,11] in relation to issues concerning on the one hand painting materials and technology and on the other painting style and thematic content. In contrast, information regarding wall paintings from later periods is scarce. The current project begins to redress the balance, and to augment our understanding of the whole palette of Cretan wall painting pigments.

The principal materials and methods of constructing a wall painting remained almost unchanged on Crete from the Bronze Age until (and in many cases including) the 20th century. Levelling layers of plaster, usually a combination of hydrated lime (calcium hydroxide) with various inorganic and organic filler materials such as calcitic or quartzitic sand, crushed ceramics, or straw, were applied to the wall, prior to the application of a thin, fine layer of almost pure slaked lime. In most cases, pigments were ground to powder, mixed with water, and applied to the still wet uppermost plaster

layer, where they would adhere to the surface through carbonation of the hydrated lime (the *a fresco* technique). Whether or not a second technique of wall painting was employed (using an organic binding medium such as egg or casein – painting *a secco*), is difficult to ascertain due to the deterioration of organic materials through time.

The most commonly found pigments in each period tend to be the 'mineral pigments', red, yellow, and the multifarious tonal variations from brown to orange to purple provided by iron oxides or hydroxides (heamatite, Fe_2O_3; goethite, FeO(OH); limonite, Fe_2O_3 xH_2O). In the Bronze Age, black pigments were charcoal based, typically created from burnt plant or bone, although some black pigments were formed from ground pyrolusite (MnO_2), while white was generally produced from calcium carbonate ($CaCO_3$) or kaolinite ($Al_2Si_2O_5(OH)_4$). Greater variation is evident in the blue and green colours, both in tems of the early and continued use of the synthetic blue pigment Egyptian blue (cuprorivaite, $CaCuSi_4O_{10}$), and the creation of hues through admixtures and layering, for example yellow over blue to achieve a green hue, and red above blue/black for purple. The introduction of synthetic lead based pigments – white ($Pb(OH)_2{\cdot}2PbCO_3$) and red (Pb_3O_4) – in the Roman period, enriched the palette, and created more vivid tones of pink and orange, although the basic palette was unchanged from the earliest Cretan wall paintings.

The diachronic approach to the project has raised interesting questions regarding the painting technologies of the different periods. Comparing the pigments employed in Bronze Age Crete to those of the Roman and Byzantine periods provides information regarding the relative importance of, on the one hand, iconographic tradition, and on the other, the more basic issues of availability/accessibility of painting materials. In addition to the appearance or disappearance of certain pigments, the use of admixtures and layering of pigments to alter their optical effects throughout the history of Cretan wall painting was studied. In this way, archaeometry, archaeology and technical art history are drawn upon to determine what materials, or combinations of materials were selected, and some of the reasons behind these choices.

From the materials characterization standpoint, the pigment study, described in this paper, follows a multi-analytical approach that explicitly makes use of a combination of non-destructive and micro-destructive techniques. Such a strategy is increasingly adopted in wall painting studies, and especially in the Aegean Bronze Age [Table 4.3 in Ref. 9]. In this study, laser-induced breakdown spectroscopy (LIBS) and Raman micro-spectroscopy, based on two compact mobile instruments, were employed for direct analysis of the wall painting fragments, complemented by x-ray diffractometry (XRD), scanning electron microscopy coupled to electron microprobe analysis and x-ray mapping, that served as reference methods providing detailed information on the pigment composition and identity. The main objective of this campaign was to investigate the applicability of LIBS and Raman techniques

and analysis of paint materials and assess the level and confidence of analytical information comparing the results with detailed materials analysis obtained by XRD.

The LIBS technique has been used in the analysis of objects of archaeological and artistic importance [12,13]. It provides information about the elemental composition on the basis of the optical emission spectrum arising from a micro-plasma that is generated by means of focusing a laser pulse on the surface of the object/sample investigated. One of the important features of LIBS is that no sampling or sample preparation is required. The analysis is carried out directly on the object. The technique is almost non-destructive, actually classified as micro-destructive, since the diameter of the spot that is probed in the analysis is of the order of 100-200 micrometers. The depth of the crater formed does not exceed a few micrometers, in the case of wall paintings (it is significantly less when hard materials, such as stone or metals are probed). In the past few years, several research groups have demonstrated that LIBS analysis can be performed using compact equipment and as a result portable LIBS units have emerged that were proved useful in the context of cultural heritage analysis [14,15,16]. The present application of LIBS has at least one point of comparison in the form of data obtained by Brysbaert et al [17] on Minoan wall paintings from Palaikastro in eastern Crete, as well as Thebes on the Greek Mainland and Tell d'Aba in Egypt of contemporary date.

Raman spectroscopy is a widely-established technique, an excellent analytical tool for art conservation and archaeological science that presents unique advantages over other molecular analysis techniques. [18,19] It features high sensitivity and specificity enabling analysis of a wide variety of organic, inorganic and bio-materials, often directly on the object under study, non-invasively, at short times and with superb spatial resolution when the analysis is performed on a Raman microscope. Raman spectra arise as a result of inelastic scattering of light by matter and display bands at frequencies, corresponding to characteristic vibrational modes of molecules or materials. These frequencies are intimately connected to the chemical bonding and its immediate environment and as such are highly specific enabling identification of various materials, for example pigments and minerals; in certain cases Raman spectra permi discrimination among different crystal phases of the same material.

X-ray powder diffraction (XRD) is a rapid analytical technique for identifying unknown crystalline phases. Normally, the analyzed material is finely ground, homogenized, and the average bulk crystalline phase composition is determined. By comparing the positions (angles) and intensities of the diffraction peaks against a library of known crystalline materials, the target material can be identified.

2. Experimental

2.1 Wall painting samples

Fragments from each of the three periods were selected for analysis from :

- the Bronze Age Palace at Knossos (c.1550-1400 BC), KN01-11;
- two large Roman buildings at Knossos, the Villa Dionysos and the Unexplored Mansion (c.1st - 2nd century AD), VD01-14 and UM01-12 respectively, and
- the Byzantine Mitropolis Basilica, at Gortyna in the south of the island (5th -6th century AD), G01-12.

Fragments were chosen with paint layers consisting of one or more of the typical pigments found in each period, or which appeared to be anomalous in terms of hue, mixtures or layering. Other selection criteria included size, condition, and relative significance of the fragments, and little/no evidence of modern conservation interventions. Initial examination under a stereomicroscope aided the selection of fragments for analysis, and refined questions to be addressed through analysis.

The archaeological/art historical focus throughout may be summarised as follows: how much continuity do we see in the practice of wall painting from Bronze Age to Byzantine Crete in terms of the materials used and the methods of applying them?

2.2 Replicas

Before beginning analysis of the wall painting samples, preliminary work was undertaken on replicas created in order to test and hone the analytical techniques. The replicas consisted of a layer of coarse lime plaster (1:3 lime and quartz sand) and an uppermost layer of lime and fine sand 2:1. Four pigments were selected: red ochre; green earth; carbon black; and manganese black, all from Kremer Pigments. For the *fresco* replicas, pigments were ground and mixed with de-ionised water at 1, 10, 20 and 40% concentration. These were applied 1 hour after application of the uppermost plaster layer to achieve optimum adherence of pigments within the carbonating lime. For the *secco* replicas, pigments were mixed at the above concentrations with a selection of organic binding media: walnut oil; lime-casein; hide glue; egg yolk and egg white; beeswax; mastic; gum tragacanth, and were applied onto the dry plaster surface.

2.3 LIBS analysis

In this campaign, a portable LIBS spectrometer (LMNT-II) was used. This instrument, developed and constructed at IESL-FORTH, is based on a small size passively Q-switched Nd:YAG laser (MK-367, Kigre Inc) producing 10 ns pulses at 1064 nm with maximum energy at approximately 10 mJ/pulse. A

dual compact fiber optic spectrograph (Avaspec-2048-2-USB2, Avantes) is used to record the emission spectra across a wavelength range extending from 240 to 760 nm, with spectral resolution of about 0.1 nm. The system is equipped with a miniature CCD camera that enables visualization of the object during analysis and aiming of the laser beam. All spectra were collected with a time-delay of 1.3 μs with respect to the laser pulse minimizing the continuum present at early times following laser ablation. In a typical analysis, the object is placed at the focal point of the focusing lens (approximately 70 mm from the optical head), and by means of a XYZ-translation stage the laser beam is aimed accurately on the point selected for analysis, which is viewed on line through the CCD camera. An area corresponding to a round spot of diameter approximately 0.2 mm is probed by the laser beam. A single pulse is adequate for obtaining a spectrum with high S/N. Typically, 2 to 3 pulses were delivered at each point in order to have a reliable representation of the paint layer composition. In some cases it has been observed that the first pulse carries information coming from surface dirt or dust. More pulses were used and consecutive single-shot LIBS spectra were recorded only when depth profiling information was sought. The latter can be achieved because of the laser ablation effect that results in the removal of a thin layer (of the order of a few microns per pulse) of material following irradiation with each pulse. (see also section 3.3)

2.4 Raman microscopy

In the present study, a mobile Raman microspectrometer (HE 785, JY Horiba) was used. The excitation source is a cw diode laser, emitting at 786 nm (maximum power on the sample : 50 mW), fiber optically coupled to an optical head that enables focusing of the beam by means of a number of objective lenses (10x, 20x, 50x) which provide variable focusing of the beam (and thus magnification of the work area) down to a few microns on the sample surface. A white light illumination system and a high resolution colour camera (video microscope) are also part of the optical head and offer very clear view of the area under investigation, necessary for positioning the beam on individual pigment particles or particle aggregates. The scattered Raman radiation is collected through the focussing objective and sent through an optical fiber to a compact spectrograph, equipped with a concave grating, which provides spectral coverage up to 3200cm^{-1} at a spectral resolution of about 10-15 cm^{-1}. Spectra are recorded on a high-sensitivity, air-cooled detector, Synapse^{TM} CCD (1024 x 256 pixels).

In a typical measurement, the entire fragment is placed under the microscope objective and with the help of an XYZ micro-positioner and the video microscope, the spot to be analysed is selected. Analysis is therefore performed in situ, namely on the fragment itself, with no need of any sampling. A limitation, we experienced with a few of the fragments, was related to the high surface roughness that prevented the high magnification objective from focusing on features that were located in “deep valleys”. The beam power on the sample was, depending on the material investigated, in the range of

0.05-5.5 mW. Typical exposure time of the CCD was 20 s per scan, while normally 10 to 20 scans were averaged.

A laboratory Raman microscope (Nicolet Almega XR) was used in a few cases when excitation at a short wavelength (473 nm) was needed, for example in the case of some blue paints that contained Egyptian Blue, which fluoresces very strongly when excited at 786 nm.

2.5 X-ray diffraction analysis

The crystalline phase analysis was carried out on a Bruker D8 Advance Diffractometer, using Ni-filtered Cu Kα radiation (35 kV, 35mA) with a Lynx Eye strip silicon detector. Data were collected for 2θ values in the range of 3° to 70° with a step size of 0.02° and a count time of 1 second per strip step. The diffractograms were taken non-destructively directly on the surface of the fragment, or by dispersing with alcohol a few milligrams of pigment material (<5 mg) on a zero background Si-sample holders. The diffractograms were analyzed and interpreted with the Diffrac Plus software package from Bruker and the Powder Diffraction File (PDF).

The size of the painted plaster fragments varied between 3x3 and 0.2x0.2 cm^2. They were rotated so as to minimize surface roughness and grain size effects (grain size should be <10 μm). Since many of the wall paintings have a layered structure, the penetration depth of the X-ray beam determines the paint thickness to be analysed. The penetration depth depends on the mass absorption factor and the density of the crystalline phases (calculated for some of the identified minerals and shown in Table 1) and is a function of the diffraction angle 2θ. Typical penetration depth values are given in Fig. 1. In samples with more than one pigment layer, the penetration depth determines the crystalline phases detected by XRD. Considering, for example, a hematite layer over a layer of Egyptian blue, both approximately 10 μm thick, and taking into account that the characteristic 2θ peaks are at 33.31° for hematite and at 11.65° and 27.10° for Egyptian blue, it turns out (according to the figures shown in Table 1) that XRD will not detect Egyptian blue lying under the hematite layer because the penetration depth in hematite for 2θ at 10° and 30° is 1.1 and 3.2 μm respectively (for Cu radiation). In the reverse case (actually encountered in sample VD08) hematite is clearly detected under a layer of Egyptian blue, whose penetration depth for 2θ at 30° is 26 μm; thus both mineral phases, Egyptian Blue and hematite, are detected.

At this point it is necessary to recognise some limitations of relying solely on XRD for the crystalline phase identifications. The first concerns minerals belonging to the mica mineral group - illite, muscovite, biotite, celadonite and glauconite – having the characteristic d-value 10Å at 2θ = 8.85° (CuKα). But this peak in illite, celadonite and glauconite is broad compared to that in muscovite and biotite. Since both celadonite and glauconite are characterized as Green Earth it is important to be able to differentiate them, and so additional criteria, those of colour and especially chemical composition,

are introduced. Celadonite and glauconite are very similar in chemical composition, especially in their Fe content, but the former is usually richer in Si and Mg and poorer in Al than glauconite. The situation regarding riebeckite, which features commonly in our results, constitutes the second limitation: this mineral shares the same main peak of $2\theta=10.7^{o}$ with d=8.3Å with other members of the amphibole mineral group such as tremolite, actinolite, hornblende and glaucophane. Again, chemical composition data is required to resolve the identity of the mineral. To this end, polished sections were prepared of a number of specimens, which were subsequently examined by optical microscopy and scanning electron microscopy (SEM).

Please insert Table 1

Please insert Fig. 1

2.6 Optical microscopy

Polished cross-sections of the minute wall painting samples, containing all the microstratigraphy from the pigment to the plaster substrate, were prepared and studied with an optical polarizing microscope in reflected light for the following: colour, particle size, shape, pigment/binding medium ratio, as well as on the thickness of paint layers, admixtures of pigments, and paint layer stratigraphy. This offers a useful 'pictorial' guide when interpreting data from elemental analyses. In the present study, images of cross sections were particularly instructive in the interpretation of results when juxtaposed with data from LIBS depth profiling, concerning successive layers of pigments; an example appears in Fig. 2. Examination of the replicas with optical microscopy focused on similar issues and included a) observation of the cross sections' autofluorescence under ultraviolet light and b) the use of staining tests for organic materials detection (Oil Red for oleaginous [20] and fluorescein isothiocyanate for proteinaceous [21,22] media respectively).

Please insert Fig. 2

2.6 Scanning Electron Microscopy (SEM)

The same samples were also analyzed on a JEOL JSM 5400 Scanning Electron Microscope, equipped with an Energy Dispersive X-ray Spectrometer by Oxford instruments (INCA energy 300 EDS). Microanalysis of single pigment grains down to 1 μm, as well as of the matrix and the total average of the paint layer were performed. Furthermore, X-ray mapping was used to study the element

distribution in the pigment layer. The above technique permitted a full micro-stratigraphic analysis and interpretation of all decorative and background paint layers and the chemical composition of the mineral pigments.

3. Results and Discussion

The overall analytical study was divided into two stages. *Stage1* concentrated on the use of LIBS and Raman micro-spectroscopy for the characterization of the painted plaster fragments (a total of 53) involved in this study. As detailed in the experimental part, both techniques carry out spot analysis, and in the case of polychrome samples several spots across the painted surface were analysed. The main goal of Stage 1 studies was to evaluate the capability of the LIBS and Raman techniques for obtaining analytical information *in situ*, involving zero sample preparation. This is of particular importance considering that both techniques are portable and therefore can be used for analytical campaigns that are performed on site. *Stage 2* studies were based on the use high performance laboratory instruments such as XRD and SEM-EDX that enable a thorough characterization of the paint and identification of its constituent pigment minerals. These measurements were performed on a smaller, but representative number of fragments that were selected on the basis of the results obtained in Stage 1, and provided further grounds for critically assessing the results obtained by the LIBS and Raman analyses.

To facilitate the discussion, analytical results are presented, grouped on the basis of paint colour, following the stage1-stage 2 approach outlined above. Furthermore, the overall analysis results are discussed in terms of their significance concerning pigment materials used across the different historical periods investigated.

3.1 Red

This group involves several wall painting fragments, a total of 21 (Table 2), exhibiting different tonalities of red (from dark to light) and pink; in some cases the paint layer extends all over the painted surface, while in others it covers just a fraction of it being part of a polychromatic motif. In all fragments, independently of site or period, LIBS spectra collected on the red paint show emission lines corresponding to iron that provide strong evidence for the presence of an iron-based pigment that is most likely a red ochre (typically composed of Fe-oxides/hydroxides, clay, quartz, calcite). A number of additional elements, such as Ca, Na, Al, Mg, Si, but also Ba and Sr in trace concentration and occasionally Zn, are also detected based on distinct emission lines observed in the LIBS spectra. These obviously originate from matrix minerals such as, for example, calcite, clay minerals and quartz, and have been detected in all fragments examined. A positive correlation between Sr and Ca due to the substitution of Ca by Sr in the calcite crystal structure is observed in all cases in which Ca was detected. A representative LIBS spectrum from a red painted plaster is shown in Fig. 3. Strong

emission lines from Fe and Ca are clearly observed, while lines from Na, Al, Mg, Si, Ba, Sr and Zn are easily identified.

Please insert Fig. 3

From the qualitative point of view, identifying Fe in a red painted plaster is a rather trivial finding, given that red ochre was commonly used in antiquity including the Byzantine period relevant to this study. But something that can be further evaluated is the Fe emission signal intensity. This depends on the concentration of Fe in the sample and in general can be correlated with the pigment density. In this context it is instructive to view as an example the average intensity of the same Fe emission line recorded in all plaster samples that were examined as a function of paint colour. (Fig. 3) Despite rather significant line intensity variations among the different samples, it is relatively straightforward to discriminate high Fe-content paints, mainly red and ones from those of low Fe-content. The high Fe-content found in yellow, brown or red coloured paints is a strong indication for the presence of iron-oxide-hydroxide minerals, but, obviously, unambiguous pigment identification is given by the XRD or Raman analysis. It is further interesting to observe that non-red or non-yellow paints still contain amounts of iron that most likely relate to Fe-containing minerals present in the plaster or used as pigments. This observation is to be further discussed in the context of the blue, green and black paint analysis.

Returning to the observed line intensity variations, it has to be noted that matrix composition is an important factor that determines the overall signal intensity in a LIBS measurement. Thus spectral lines, such as for example those shown in Fig. 3, have to be taken into account cautiously as regards correlation of their intensity with the concentration of a certain element in the solid and spectral emissions should be considered as representing a semi-quantitative picture.

Please insert Fig. 4

Continuing with the LIBS analysis of the red plaster fragments, an interesting observation is the clear presence of lead, Pb, in the red paint in a small number of samples, two from Gortyna (G03, G06, Roman – Byzantine period) and one from the Villa Dionysos at Knossos (VD01, Roman period) (Fig. 5). The origin of Pb emission, which can be related either to red lead (minium, Pb_3O_4) or lead white ($Pb(OH)_2 \cdot 2PbCO_3$), is a question to be addressed by the molecular analysis techniques employed in the present study. However, it is noted here that the presence of Pb in sample G03 was also confirmed through X-Ray mapping performed on a polished cross section in SEM, which clearly indicates that

Pb is rather diffusely distributed across the paint surface in a manner similar to that of Ca and clearly different from the more localized distribution of Fe, Al and Si. This may suggest that the red pigment is an iron-based one, while the presence of Pb relates to lead white used as a background or in order to dilute the red paint. This is in agreement with a further observation, made on the basis of LIBS data, proving that Pb is present in the blue and black paint of fragment VD01, besides the red paint as well as in the blue paint of fragment G01. From the perspective of materials use and availability it is important to note that Pb was detected solely in samples from the Roman and Byzantine periods and not in ones from the Bronze Age.

Please insert Fig. 5

In parallel to LIBS analysis, Raman spectra were collected from 21 red painted plaster fragments, of which 13 showed spectral bands characteristic of red iron oxide, Fe_2O_3 (hematite). This clearly proves the presence of hematite/red earth and effectively confirms the strong evidence provided by the LIBS data. For example, in Fig. 6 indicative Raman spectra collected from red painted plasters from the sites of Knossos (VD10) and Gortyna (G04) are shown against a spectrum collected from pure red iron oxide. Raman bands at 229 cm^{-1} (A_{1g}), 296 cm^{-1} (E_g) and 412 cm^{-1} (E_g) correspond to Fe_2O_3 vibrations modes.

Please insert Fig. 6

As mentioned in the experimental part, a major advantage of Raman microscopy is that, by focusing the laser beam on distinct pigment grains or pigment-rich areas, one may avoid excitation of other co-existing pigments or impurities thereby minimizing unwanted interferences. Indeed this has been the case throughout this study, yet it is interesting to note that a number of red painted plasters did not yield spectra corresponding to hematite or any other red pigment, despite efforts to focus on red pigment grains/areas. Instead, broad features due to fluorescence were observed and, in some cases, bands related to the presence of calcite, gypsum or quartz (Fig. 7). These observations are attributed to the fact that the Raman analysis is conducted *in situ* without any surface/sample preparation (e.g. polishing), thereby suffering limitations that relate either to excessive contribution of fluorescence from impurities or organic constituents or to inefficient exposure of the relevant pigment grain or grains to the laser beam when other, often transparent, minerals are masking the pigment. It is noted that calcite bands were recorded in several of the samples examined (see Tables 3-6), independent of plaster colour. This observation may be possibly due to a) the use of lime white to modify or extend

(dilute) the pigments, b) the presence of impurities in the raw material [23] or c) contributions to the Raman signal from the lime plaster substrate. It is recalled that strong Ca emission lines were detected in all LIBS spectra as well.

Raman spectra collected on those red plaster fragments, which by LIBS analysis were found to contain Pb (VD01, G03, G06), showed no bands coming from either red lead or lead white (expected at 122, 148, 550 cm^{-1} or 681, 1051 cm^{-1} respectively). [24] No hematite bands were observed either. Instead, the presence of calcite was verified by its strong band at 1089 cm^{-1}, in G03 and G06 (Fig. 7) while VD01 showed just a very strong fluorescence background. It is noted that measurements in these samples were mainly limited to red areas and no spectra were collected from white areas, where the probability of finding lead white would have been higher. Furthermore, given that lead white is present at relatively low quantities compared to calcite, as shown by LIBS, any Raman signal, expected at 1051 cm^{-1} would be low and possibly masked by the nearby strong band of calcite at 1089 cm^{-1}.

Please insert Fig. 7

A representative number of red painted plasters was analysed by XRD (KN09, UM04, UM08 and VD10) and on the basis of the characteristic diffraction peaks recorded, the presence of hematite was confirmed. In addition calcite, illite, kaolinite and quartz were detected, which could be primary accessory minerals in the iron ochre pigments. As regards calcite, it is added that it is also as secondary mineral by the carbonization of slaked lime used in the fresco painting technique. The XRD results reveal the identity of the minerals in the red paints examined and essentially help to explain the LIBS data, which, besides Fe, arising from the red ochre, show additional elements related to the accessory minerals of the pigment. Likewise, Raman data are in good agreement with the XRD results. It is noteworthy that in UM04 tridymite, a high temperature polymorph of SiO_2, was identified by XRD, a clear indication for the presence of synthetic hematite, produced by heating a Fe-hydroxide ochre.

Please insert Table 2

Further analysis of wall painting pigments from the Roman period onwards may reveal a more varied palette, however, on the basis of results from the current study it seems that painters in Crete adhered to a more traditional range of materials than were used elsewhere. This is seen especially with the red pigments. The Roman writers Pliny and Vitruvius [25,26,27] refer to various red pigments other than

the iron oxides found in the Cretan examples discussed here, including red lead (lead tetraoxide), cinnabar (mercury sulphide; Ref 26, pp. 119-127), and realgar (arsenic sulphide; Ref. 26, pp. 75-77). Analysis to date indicates that lead based pigments were not part of the Bronze Age Cretan wall painting palette. Red lead is less attested historically than lead white, although it is included in Pliny's list of pigments (Ref. 25, p.119, p.123, p.217, pp.220-1), and was reported in paintings again from Pompeii [28]. Although much later in date, it is interesting to note that painters are cautioned by the early 15th century writer Cennino Cennini [29] (in Chapter. XLI) against the use of red lead as a wall painting pigment due to its chemical instability.

Cinnabar (HgS) has been identified in Hellenistic and Roman painting, both as a pure pigment (as at Vicenza [30] and Pella, Greece [31]) and as admixture with red ochre (in Cyprus [32]). The organic red colorant madder, deposited onto an insoluble base, has also been identified in the Pompeian paintings [23].

3.2 Yellow

As with red, LIBS analysis of yellow paint, carried out on a total of seven plaster fragments (Table 3), resulted in intense emissions from Fe in the corresponding spectra (see also Fig. 3) which correlate with the expected presence of yellow ochre (goethite or limonite).

Based on the Raman spectra (Fig. 8) that were collected from VD09, VD10, UM07 and UM10, clear information about the identity of the yellow pigment is obtained on the basis of characteristic spectral bands of goethite, FeO(OH). It is noted that yellow ochre, named also limonite ($Fe_2O_3 \cdot xH_2O$) is almost amorphous while goethite is crystalline. As was found with the red paints, Raman spectra collected on two yellow paints yielded no goethite bands neither bands corresponding to limonite, which is found in yellow ochre. XRD analysis indeed confirms the presence of iron oxide minerals in the yellow painted plasters (hematite in KN08, VD09 and geothite in VD10).

Please insert Fig. 8

Analysis of yellow paint layers from both the Bronze Age and the Roman period have identified pigments based on iron oxides, yellow ochre. Although a second yellow pigment, orpiment (arsenic sulphide), is mentioned by both Pliny and Vitruvius (Ref. 25 p.101; Ref. 27 : Vitruvius VII, Chapter VII), Pliny notes the unsuitability of orpiment as a pigment for fresco painting, and definitive identification of its use in Roman wall painting is lacking [33]. Despite the increasing application of

lead based yellow pigments from the Roman period onwards (for example, the lead oxide pigment massicot has been identified in Roman paintings at Pompeii, while in later artists' treatises, such as *Il Libro dell' Arte,* Cennino Cennini describes a (presumed) lead tin yellow pigment he names Giallorino (Ref. 29: Ch. XLVI)), painters in Crete appear to have maintained the more traditional palette, and continued with the use of yellow ochre.

Please insert Table 3

3.3 Blue

Blue paint was present in 21 of the plaster fragments investigated (Table 4). Notably, in 14 of these fragments LIBS spectra record relatively weak but clear emission from Cu indicating the use of a Cu-based blue pigment that cannot be further identified on the basis of its elemental composition.

Please insert Figure 9

Despite the fact that the blue colour on the plaster surface is very clear and in some cases quite vivid, it is surprising that the Cu emission signal observed in some of the LIBS spectra is rather weak. Observation of the blue paint under the optical microscope shows clearly the presence of a rather low density of relatively large-sized dark blue pigment grains scattered across a white matrix background. Evidently this particle density is adequate to yield a blue colour appearance to the paint. But in the LIBS measurement, the focused laser beam probes, along with the few pigment grains, a significant part of the lime-based matrix, leading to an emission spectrum that represents the average composition of the area analysed (of diameter in the range of 150-200 μm), which is dominated by the strong Ca emission lines (Fig. 9).

LIBS was found to be particulalrly effective in the characterization of layered paints. When LIBS analysis is performed by using a number of consecutive laser pulses on the same spot, corresponding spectra from successive layers of material can be recorded, that map the in-depth composition of the paint layer or layers. This can be considered, in a way, as a kind of direct/in situ cross-section analysis. One however needs to take into account two issues: a) the thickness of material removed per laser pulse (λ = 1064 nm) is of the order of 1 micron, yet this can occasionally become significantly larger when fragile paints are analysed and b) each pulse still monitors an average composition across the irradiated spot (diameter approx. 150-200 μm).

For example, optical inspection of wall painting fragment VD08 showed clearly that at some point the red paint has been applied over an underlying blue layer. LIBS analysis was carried out at that area employing a total of 7 laser pulses and recording (single-shot) spectra corresponding to each individual pulse. By monitoring the Cu line intensity, (Fig. 10) a transition point is clearly observed following irradiation of the paint with the fifth laser pulse. Evidently a gradual layer-by-layer removal of paint takes place revealing the Cu-rich underlying paint. It is noted that Cu is detected from the very first pulse, albeit at rather low intensity, until reaching pulse number 4, indicating that either small quantities of the blue pigment are present in the red paint or that the red paint particle density is such that it permits part of the laser beam to reach the underlying blue paint layer. On the other hand, considering the Fe-line(s) intensity, it is seen that the Fe emission signal does not change dramatically. It is noted that the low signal corresponding to the first pulse, has been observed in several other fragments as well, and is attributed to inefficient plasma formation resulting when a fresh surface, bearing loose dust or particles is irradiated. Finally, pulse number7 shows a decreasing trend that might indicate a drop of Fe concentration when the beam finally reaches the blue paint layer. In the same wall painting fragment, a purple paint over blue was also investigated in the same fashion, a total of eight laser pulses were used, giving quite similar results with the Cu-line intensity showing an increase upon reaching the blue paint layer and the Fe-line intensity correspondingly decreasing.

Please insert Figure 10

Raman measurements on the blue paints were quite revealing and in most cases enabled identification of the Cu-based pigments suggested by LIBS. In particular, 11 of the 13 blue plaster fragments examined, all from Knossos, were found to contain Egyptian Blue ($CaCuSi_4O_{10}$, cuprorivaite). Notably the Egyptian Blue identification was based not on any Raman bands but on the extremely strong fluorescence emission recorded when the microscope objective was focused on blue pigment grains or grain aggregates (Fig. 11). It is widely known [34,35] that Egyptian Blue, upon excitation in the visible and NIR, exhibits strong fluorescence emission with a maximum at about 890 nm.

Please insert Fig. 11

Unlike the samples from Knossos, those from Gortyna showed neither Egyptian Blue fluorescence nor any Raman bands that could be related to the presence of a different blue pigment. It is noted here that azurite, a Cu-based blue pigment, known to have been used in Byzantine times, shows quite low

Raman scattering cross-section when excited in the NIR, i.e. 786 nm [36] and therefore might escape detection. Surprisingly, in two cases, G11, G12, for which LIBS spectra did show the presence of Cu, Raman bands characteristic of phthalocyanine blue ($CuC_{32}H_{16}N_8$) were recorded. (Fig. S1 in the Electronic Supplementary Material) Considering that this Cu-based synthetic pigment was introduced in 1936 it is most likely that its presence relates to some kind of recent restoration work. For example, a similar pigment, phthalocyanine green, has been found in Roman wall painting at the Vesuvius area [37] and has likewise been attributed to conservation work.

XRD analysis confirmed the presence of Egyptian Blue (cuprorivaite) in all cases. Significantly, Mg-riebeckite, a blue pigment, was also found to be present but only among some of the Bronze Age samples (Fig. 12a) along with calcite, talc (an accessory mineral of Mg-riebeckite) and quartz. The presence of Mg-riebeckite is also nicely shown in the SEM images (Fig. 13) collected from cross-sections of micro-samples from wall painting fragments KN02 (see also Fig. 2) and KN06. The images are annotated with results from qualitative elemental analysis and X-ray mapping that enable clear identification of the different mineral grains. It is noted that Mg-riebeckite was first identified as a blue pigment in the context of Bronze Age wall painting studies by Perdikatsis and co-workers. [38,39,40] Finally it is noteworthy that in sample VD08 three pigments are identified by XRD, Egyptian Blue, Hematite and Dioptase ($CuSiO_2(OH)_2$) as shown in Fig.12b.

Please insert Fig 12

Please insert Fig 13

Please insert Table 4

While the amphibole pigment Riebeckite was identified in several blue paint layers from the Bronze Age fragments, blue pigments in the Roman palette appear to be limited to Egyptian blue. This is in accordance with the main body of work on Classical/Hellenistic and Roman pigments (such as from the Hellenistic Tombs at Vergina, [41] at Lefkadia, [42] at the Roman House of Orpheus, Nea Paphos, Cyprus [32] and in the early Byzantine scheme 'Christ and 12 Apostles' from Vault 9, Caesarea. [43]

An important but unexpected find is the mineral dioptase, identified in VD08, which is a rare emerald-green to bluish green copper silicate. It occurs at Laurion but presumably also elsewhere in Greece. Its use in icon painting in Minsk, Belarus has been noted. [44] Dioptase appears in the upper oxidized portions of copper ore deposits along with malachite. In sample VD08 dioptase must have

been added as a pigment because had it been in the primary copper ore, used in the synthesis of Egyptian Blue, it would have been decomposed at the high temperature at which Egyptian blue is forming.

3.4 Green

Of the wall painting fragments examined (Table 5), green colour paint was present in 17, all belonging to the Roman to Byzantine periods. LIBS analysis of these green plasters rendered spectra having an overall elemental profile containing Al, Ba, Ca, Fe, Mg, Na, Si, Sr typical of earth materials, with the exception of fragments VD08, which, in addition showed weak emissions due to Cu. Interestingly, G08 was found to contain low amounts of Cr. While Fe line intensity values are clearly lower compared to those observed in the red and yellow paints, it appears that Fe content is statistically different from that of the unpainted plaster suggesting that some Fe-based mineral, for instance, green earth, may have been used as a pigment.

Examination of UM01, UM02, VD08 and VD09 under the Raman microscope resulted again in intense fluorescence emission spectra quite similar to those obtained from the Egyptian Blue containing blue samples (Fig. 11). It is noted that some of them, as observed under the microscope, clearly exhibit blue-coloured grains that are believed to be the origin of the strong photoluminescence observed. This result is a likely indication of mixing blue (Egyptian Blue) and yellow (yellow ochre) pigments for generating green [45]. Another six samples from Knossos and all those from Gortyna showed no evidence for Egyptian Blue, nor did they have Raman bands distinctive of any green pigment.

Returning to the LIBS results that apparently have failed to detect Cu in most of the green plaster samples, in which Raman analysis proved the presence of Egyptian Blue, except in VD08, the effect is again attributed to the different magnification of the two systems already discussed in the blue paint analysis section.

Interestingly, XRD analyses have confirmed the presence of Egyptian blue in most of the green painted plaster samples (UM01, VD08 and G09). This is strong evidence that green colour has been created by mixture of Egyptian Blue with some yellow paint. In one case, G08, the green colour can be attributed to the presence of glauconite. (Fig. 14) Also, the presence of a chromite grain in or adjacent to the celadonite is interesting given that this co-existence has been reported in celadonite from Cyprus.[46,47] Importantly, LIBS has detected Cr in the green paint of G08.

Please insert Fig. 14

Please insert Table 5

While the layering of blue and yellow pigments to achieve a green colour is attested in Bronze Age Aegean painting (amphibole blue above yellow ochre at Thera, [39]) that this practice continued in the painting of later periods is surprising. This admixture has been identified in Roman paintings from Acre, Israel [48], however, according to analyses green earth is much more typical during this period. Since green earth was identified (G08), yet seems to have been used infrequently, one may hypothesise that the more vibrant tone offered by the admixture of Egyptian blue and yellow ochre rendered this a more desirable option. Interestingly, Egyptian blue was found in combination with green earth at Brescia, Italy [49], presumably to enrich the hue of the green pigment. Other green pigments known during the Roman period, according to primary sources and analyses, malachite ($CuCO_3{\cdot}Cu(OH)_2$) and verdigris ($Cu(CH_3COO)_2$) [33], are less commonly found, and appear to be absent from the Cretan palette.

3.5 Black and grey

LIBS spectra collected on the black and grey painted plasters show strong emission lines coming from Al, Ca, Na, and Si, while Fe shows significantly weaker emission compared to the red and yellow paints. This weak Fe emission suggests the total absence of black iron oxides (Fe_3O_4) and indirectly points towards the use of a carbon-based black pigment. However, the presence of carbon cannot be unambiguously verified by LIBS under the measurement conditions used in this campaign. In one of the samples from Gortyna, G01, relatively strong emission lines from Mn and Pb were observed in the LIBS spectrum (Fig. 15). The presence of Mn is strong evidence for the use of a Mn-based black pigment, most likely pyrolusite, MnO_2, while Pb is related to the presence of lead white. In the same spectrum a weak signal from Cu is also recorded that could be related to the presence of a small quantity of a Cu-based blue pigment either added intentionally to modify the colour or accidentally introduced as an impurity. Copper was likewise found in VD01. It is also recalled that red paints in G06 and G10 were found containing small amounts of Mn, most likely as impurities from nearby paints.

Please insert Fig. 15

Grey and black paints examined by the Raman microscope failed to yield meaningful spectra, one of the reasons being that excitation in the NIR (786 nm) is not appropriate for analysis of black pigments (even neat manganese black or bone black gave no Raman bands in our spectrometer). It is noted

however that several grey (KN06, UM10) and purple paints (UM07, VD08) when examined under the microscope revealed clearly the presence of blue grains and when analysed resulted in the characteristic fluorescence emission of Egyptian Blue, observed in blue paint. The black in UM05 is shown in Figure 16.

Please insert Table 6

Please insert Fig. 16

Throughout the ages, black colours were typically created with carbon black (from burnt vegetal matter, or, more rarely, bone). A black mineral pigment, manganese oxide, has been identified in wall paintings from the Bronze Age (at Phylakopi on Melos and at Orchomenos, [50]), to the Roman period (at Nea Paphos, Cyprus, [32]), although carbon based black pigments were much more commonly used in all periods. The occurrence of amphibole blue pigments within a predominantly carbon paint layer, seen in several samples here from Bronze Age Knossos, is paralleled with findings from Akrotiri, Santorini. [39] This was probably to alter the hue, to create a dark blue-grey effect.

3.6 White

White was applied as a pigment on only one of the fragments examined in this study, VD09, in which a fairly thick layer of white paint, with good covering power, overlies a yellow paint layer. In a few other fragments white areas are present coming from unpainted plaster. In all cases, LIBS analysis showed Ca to be the dominant element. This is strong evidence that in all cases examined, the white color is lime based. It is interesting to note that in samples VD09 and UM10 traces of copper are detected in the white areas. In the case of VD09 this is clearly related to the adjacent blue and green layers that contain Egyptian blue (Tables 4 and 5). In the case of UM10 the presence of copper relates most likely to dark particles present in the plaster confirmed to be Egyptian blue (Table 6). As already noted in section 3.1 lead white appears to have been used in several of the Gortyna wall paintings (Table 2) and in one from Villa Dionysos, VD01. Lead white occurs in Hellenistic paintings in Macedonia, [51,52] and is also listed as a pigment by the Roman authors Vitruvius (Ref. 27, Book VII, p. 12) and Pliny the Elder (Ref. 26, p. 75), and has been identified in Roman wall paintings at Pompeii, [53] and at Vicenza. [54]

3.7 Modern replicas

The value of the observations on the modern replicas, introduced in section 2.2, lies chiefly in the enquiry into the painting technique which will be the object of a separate publication. Here we present only a summary of some of the findings. While the two black paint layers appeared fairly homogeneous, the green earth consisted of particles of various hues including red and orange. White particles, probably from the plaster layer, were observed in the red earth paint layers.

A distinct difference was observed between the fresco and secco paint layers with the highest concentration of pigment. While the fresco paint layers varied in thickness and presented a rather uneven surface topography, those applied with binding media were of a more consistent thickness. This was especially the case with pigment applied with egg as a binding medium.

Surprisingly, pigment penetration into the plaster layer, with both the fresco and the secco replicas, was minimal. Further experiments were undertaken mixing the pigments with saturated lime water prior to application; this resulted in deeper penetration of the pigments, but also a drastic alteration (dilution) of the pigment hue.

A distinct autofluorescence was observed in the secco paint layers containing proteinaceous binding media. Fluorescence intensity was lower or even absent in the paint layers with oil or resin respectively, most likely because of the materials having been recently applied. It is known [55,56] that in some materials fluorescence emission increases with aging. In almost all cases, some areas within the plaster layers auto-fluoresced. Staining tests for proteins and lipids detection gave positive results in the secco paint layers and false positive results in all the plaster layers.

3.8 Organic binding media

The recent positive identification of an organic binder on wall painting fragments at the Mycenaean palace at Pylos in the SW Peloponnese is relevant to our enquiry. As reported by Brecoulaki *et al* [57] by use of pyrolysis gas chromatography-mass spectrometry (PY/GC-MS) and GC-MS, Colombini and Bartolucci have detected the presence of egg, animal glue, and tragacanth gum, indicating the use of various tempera techniques at Pylos. This is an important result because it overturns previous thinking on the nature of the painting technique in the prehistoric Aegean. [Ref.10, 217f] It is generally accepted that the tempera technique was employed in Roman times.

The non-destructive approach adopted in our work yielded mixed results. There was ambiguity in the results of the staining and fluorescence experiments on the replicas (section 3.7), and their analysis with the portable Raman system failed to detect an organic component or provide good quality spectra for pigments. However the already well-known applicability of bench-top Raman to pigment and organic media analysis [19,58] was confirmed, establishing the potential of the approach to identify organic components on wall painting surfaces. Raman spectroscopy, performed on the replica samples, with excitation at 785, 613 and especially 514 nm can identify the presence of absorption

peaks of organic material but has difficulty detecting the peaks that would make it possible to distinguish between different organic binders.

4. Conclusions

In this study 53 wall painting samples were analysed in the context of a scientific study aimed at a) determining similarities and evolutions of painting materials and technology in Bronze Age, Roman-Hellenistic to Byzantine Crete and b) testing a multi-analytical technique methodology that combined mobile instrumentation, LIBS and Raman spectroscopy, with laboratory techniques, mainly non-destructive XRD performed directly on the wall painting fragments, but also SEM coupled to X-ray analysis and mapping performed on micro-samples.

Concerning practical aspects of analysis the LIBS system used was found to be rather more versatile compared to the Raman system based on operational factors, including sample positioning, signal intensity and hence sensitivity, immunity to ambient light and speed of data acquisition. On the other hand the Raman microscope offered superior magnification, hence high spatial resolution, but measurements needed rather long acquisition times (typically 1-5 minutes) and had to be performed in the dark. For that purpose a light-tight enclosure was used. Both instruments were used in situ, directly on the wall painting fragments. In particular, the LIBS system can be easily used to analyze large objects or structure (e.g. a wall) with the use of an appropriate support or scaffolding.

From the point of view of analytical information, LIBS yields data that relate to the elemental composition of the sample, actually a small area of the sample surface, typically 0.1 mm^2. Major, minor and, in favourable cases, trace elements can be detected. In the absence of proper calibration standards, quantitative results are difficult to obtain. But in cases of highly heterogeneous materials, such as those dealt with in this study, the semi-quantitative picture can still be quite useful. Actual molecular structure information cannot be extracted, however, knowing types of materials that might be present in the sample, it is often possible to correlate elemental information with specific compounds, for example iron with hematite in the case of the red paints or manganese with pyrolusite in black paints.

On the other hand, Raman spectra provide clear evidence for the presence of specific molecular structures, thus revealing the identity of pigments and minerals. Emission of fluorescence can be a source of interference, as was shown in several cases in this study, overwhelming the Raman scattering signal, which is inherently much weaker compared to fluorescence. Yet in a few favourable cases, for instance, that of Egyptian blue, fluorescence emission can offer equally valuable analytical information. Using excitation at longer wavelengths, in the near infrared, minimizes fluorescence from organic substances present but on the other hand certain materials, for example Cu pigments or carbon black are detected efficiently only with visible excitation. Finally, unlike LIBS, which results

in small but finite sample removal during analysis, the Raman technique is totally non-destructive, provided no excessive laser power is used during measurements that might lead to local thermal alteration of the sample surface.

The two techniques offer complementary information that can be quite useful for conservators and archaeologists. In addition, they feature significant advantages having to do with their application outside the research laboratory in an effective manner that enables quick surveying of samples and objects, aiding object selection for subsequent analysis by advanced laboratory techniques. These techniques include those used in this study, XRD and SEM-EDX that proved, in most cases, unambiguously the identity of pigments and minerals present in the painted plaster.

In the archaeological context, looking at data obtained on *Bronze Age,* i.e. Minoan wall paintings elsewhere on Crete, there is a high level of comparability (Ref. 9, Table 6.7a; Ref.10, Table 13.2). The presence of the green earth celadonite together with chlorite in a green fragment at Palaikastro is noted. Turning to the pigments responsible for blue colours, an issue that has attracted much attention, there are some significant geographical trends: at Knossos Egyptian Blue and Riebeckite occur sometimes together [59], as they do at Chania in the west of Crete [60], yet Egyptian Blue is absent at Kommos in the south [11] and at Palaikastro in the east. However, the situation in the Mesara of Crete appears complex since Perdikatsis [61] and Dandrau [62] have both detected Egyptian Blue in conjunction with riebeckite-glaucophane at Ayia Triadha, and at nearby Phaistos Duell and Gettens [63] found Egyptian Blue. Jones' recent attempt [64] to classify Minoan pigments as local, regional and exotic, has placed the iron-rich blue, belonging to the amphibole family and comprising riebeckite, glaucophane or crossite, as a regional product. This has followed on the geological work of Seidel *et al* [65] who recognised that, the locations of these minerals on Crete are known only at the broad geological level: glaucophane in phyllite-quartzite rocks in West Crete and crossite/magnesio-riebeckite in similar formations in the centre and east (Fig. S2 in Electronic Supplementary Material). The apparent absence of tin (note that Sn if present is certainly <1% and often <0.1%) in any of the Egyptian Blue examples studied here seems to contrast with the situation found elsewhere (Ref. 9 pp. 134-5).

On the basis of evidence from the current study, the wall painting palette used in Crete from the Bronze Age to the early Byzantine period appears somewhat limited. Few changes are seen in the materials and techniques from the earliest to the latest of our examples. Significant additions to the Bronze Age palette during the later periods are the lead-based pigment detected in some paint layers from the Roman wall paintings, and celadonite, green earth, on one Byzantine fragment. The results presented here are in accordance with previous analyses of Bronze Age wall painting in Crete and the Aegean. Likewise, results from the Roman wall paintings are consistent with those from the Roman world, but do not include any of the more 'exotic' materials, such as malachite and cinnabar, occasionally evidenced elsewhere from this period. Comparanda for the early Byzantine paintings are

apparently unavailable, but it is hoped that future research in this area will develop these preliminary findings, and provide a more complete picture of the materials and techniques used in that period.

Finally, a brief comment can be made on the plaster substrate which was found, as expected, to be lime-based in all samples. In the SEM, primary and secondary calcite was observed in eight samples. But work could usefully be done on a fuller characterisation of the plasters, including an explanation for the grey-blue hue of the plaster layer in UM10 and in a Bronze Age sample from Mochlos in East Crete containing small particles of carbon within the plaster matrix. The source of that carbon – bone ash or plant – and its purpose (colourant?) are as yet unclear. Another issue is the complex plaster stratigraphy observed in several samples, as mentioned at the start of the Results section. Along with the study of the modern replicas, this topic will be reported in a separate publication.

Acknowledgements

This project is carried out in the frame of a collaboration between the Department of Archaeology, University of Glasgow and IESL-FORTH, funded in part by the Leverhulme Trust, UK. We are very grateful to those who gave permission to analyse the wall painting fragments from their excavations: Dr Sara Paton, Dr Colin MacDonald, and Prof.ssa Raffaella Farioli. Many thanks also to all who facilitated the study and selection of original materials: Dr Doniert Evely, Professor Todd Whitelaw, Dr Evangelia Kiriatzi, Mrs Helen Clark, and Mrs Vicki Tzavara of the British School at Athens, Dr Kostas Giapitsoglou and colleagues at the 13th Ephorate of Byzantine Antiquities, the 23rd Ephorate of Prehistoric and Classical Antiquities, Dr A.G.Benvenuti, and colleagues at the Scuola Archeologica Italiana di Atene. PS and AF acknowledge support from the EC Charisma project (FP7-INFRA-Grant agreement no: 228330). We thank Prof. N. Chaniotakis in the Chemistry Department at the University of Crete, Dr Ross Stevenson and Dr Karen Faulds in the Chemistry Department at Strathclyde University and Prof. R. J. H. Clark in the Chemistry Department at the University College London for granting access to their Raman spectroscopy instrumentation.

References

1. Price TD, Burton JH (2011) An Introduction to Archaeological Chemistry, Springer, New York.
2. Ciliberto E, Spoto G (Eds.) (2000) Modern analytical methods in art and archaeology, Chemical Analysis, A series of monographs on analytical chemistry and its applications, J.D. Winefordner (Ed.), Wiley, New York, vol. 155
3. Uda M, Demortier G, Nakai I eds (2005) X-rays for Archaeology, Springer
4. Stuart BH (2007) Analytical Techniques in Art Conservation, Wiley, West Sussex, UK
5. Kockelmann W, Pantos E, Kirfel A (2000) Neutron and synchrotron radiation studies of archaeological objects In: Creagh DC, Bradley DA, eds, Radiation in Art and Archaeometry, p. 1-33, Elsevier Science., New York
6. Janssens K (2011) Synchrotron Radiation in Art and Archaeology, J. Anal. At. Spectrom. 26: 833-4
7. Abe Y, Nakai I, Takahashi K, Kawai N, Yoshimura S (2009) On-site analysis of archaeological artifacts excavated from the site on the outcrop at Northwest Saqqara, Egypt, by using a newly developed portable fluorescence spectrometer and diffractometer, Anal. Bioanal. Chemistry 395: 1987-96
8. Vandenabeele P, Weis TL, Grant ER, Moens LJ (2004) A new instrument adapted to *in situ* Raman analysis of objects of art, Anal. Bioanal. Chem., 379: 137–142
9. Brysbaert A (2008) The Power of Technology in the Bronze Age Eastern Mediterranean. Monographs in Mediterranean Archaeology. Equinox, London
10. Jones RE, Photos-Jones E (2004) Technical studies of Aegean Bronze Age wall paintings: methods, results and future prospects. In: Aegean Wall Paintings: a tribute to Mark Cameron. British School at Athens, London, pp 199-228
11. Dandrau A, Dubernet S (2006) Plasters from Kommos: A Scientific Analysis of Fabrics and Pigments. In: Kommos V: The Monumental Minoan Buildings at Kommos. Princeton University Press, Princeton, pp 236–241
12. Anglos D (2001) Laser-Induced Breakdown Spectroscopy in Art and Archaeology. Appl Spectrosc 55:186A-205A
13. Giakoumaki A, Melessanaki K, Anglos D (2007) Laser-induced breakdown spectroscopy (LIBS) in archaeological science—applications and prospects. Anal Bioanal Chem 387:749-760-760

14. Cunat J, Palanco S, Carrasco F, Simon MD, Laserna JJ (2005) Portable instrument and analytical method using laser-induced breakdown spectrometry for in situ characterization of speleothems in karstic caves. J Anal At Spectrom 20:295-300

15. Fortes FJ, Cunat J, Cabalin LM, Laserna JJ (2007) In Situ Analytical Assessment and Chemical Imaging of Historical Buildings Using a Man-Portable Laser System. Appl Spectrosc 61:558-564

16. Agresti J, Mencaglia A, Siano S (2009) Development and application of a portable LIPS system for characterising copper alloy artefacts. Anal Bioanal Chem 395:2255-2262

17. Brysbaert A, Melessanaki K, Anglos D (2006) Pigment analysis in Bronze Age Aegean and Eastern Mediterranean painted plaster by laser-induced breakdown spectroscopy (LIBS). J Archaeol Sci 33:1095-1104

18. Smith GD, Clark RJH (2004) Raman microscopy in archaeological science. J Archaeol Sci 31:1137-1160

19. Vandenabeele P, Edwards HGM, Moens L (2007) A Decade of Raman Spectroscopy in Art and Archaeology. Chem Rev 107:675-686

20. Mazzeo R, Prati S, Sandu I, Spring M (2009). Paint layers. In: Pinna D, Galeoti M, Mazzeo R,. Scientific Examination for the investigation of Paintings. A Handbook for Conservator – Restorers, Firenze Italy: Centro Di della Edifirmi srl

21. Ioakimoglou E (2010) Organic Materials in Art and Archaeology Vol. B: Proteinaceous materials in painting (in greek) Ion editions, Athens, pp. 192-195

22. Schaefer S (1996) Fluorescent staining techniques for the characterization of binding media within paint cross-sections and digital image processing for the quantification of staining results. In: Bakkenist T et al. eds, Early Italian Paintings: Techniques and Analysis, Symposium, Maastricht, 9-10 October 1996. Maastricht: The Limburg Conservation Institute Distributed by Archetype Publications: pp 57-63.

23. Eastaugh N, Walsh V, Chaplin T, Siddall R (2004) The Pigment Compendium: A Dictionary of Historical Pigments. Elsevier Butterworth-Heinemann, Oxford

24. Burgio L, Clark RJH (2001) Library of FT-Raman spectra of pigments, minerals, pigment media and varnishes, and supplement to existing library of Raman spectra of pigments. with visible excitation, Spectrochim Acta A 57:1491-1521

25. Bailey K (1929) The Elder Pliny's Chapters on Chemical Subjects, Part I. Edward Arnold & Co, London

26. Bailey K (1932) The Elder Pliny's Chapters on Chemical Subjects, Part II. Edward Arnold & Co, London

27. Vitruvius, The Ten Books on Architecture. (1960) (trans: Morgan MH). Dover Publications, New York

28. Augusti S (1967) I colori pompeiani. De Luca Editore, Rome

29. Cennino D' Andrea Cennini. The Craftsman's Handbook. The Italian "Il Libro dell' Arte". (1960) (trans: Thompson DV). Dover Publications, New York

30. Mazzocchin GA, Agnoli F, Salvadori M (2004) Analysis of Roman age wall paintings found in Pordenone, Trieste and Montegrotto. Talanta 64:732-741

31. Calamiotou M, Siganidou M, Filippakis SE (1983) X-Ray Analysis of Pigments from Pella, Greece. Stud Conservat 28:117-121

32. Kakouli I (1997) Roman wall paintings: a scientific investigation of their technology, in: Bearat H et al, eds, Roman Wall Painting: Materials, Techniques, Analysis and Conservation: Proceedings of the International Workshop, Fribourg, 7-9 March 1996. pp 131-141

33. Siddall R., (2006) Not a day without a line drawn: pigments and painting techniques of Roman Artists. Proceedings of the Royal Microscopical Society 2: 18-31

34. Pozza G, Ajó D, Chiari G, De Zuane F, Favaro M (2000) Photoluminescence of the inorganic pigments Egyptian blue, Han blue and Han purple. J Cult Herit 1:393-398

35. Accorsi G, Verri G, Bolognesi M, Armaroli N, Clementi C, Miliani C, Romani A (2009) The exceptional near-infrared luminescence properties of cuprorivaite (Egyptian blue). Chem Commun 23:3392-3394

36. RRUFF™ Project. http://rruff.info/.

37. Aliatis I, Bersani D, Campani E, Casoli A, Lottici PP, Mantovan S, Marino I-G, Ospitali F (2009) Green pigments of the Pompeian artists' palette. Spectrochim Acta A 73:532-538

38. Filippakis SE, Perdikatsis B, Th. Paradelis (1976) An analysis of blue Pigments from Greek bronze age. Stud Conservat 21:143-153

39. Perdikatsis V, Kilikoglou V, Sotiropoulou S, Chryssikopoulou E (2000) Physicochemical characterisation of pigments from Theran wall paintings. In: Sherratt S. ed., The Wall Paintings of Thera - Vol. 1: Proceedings of the First International Symposium, Athens, 30 August - 4 September 2000. pp 103-129

40. Profi S, Perdikatsis B, Filippakis SE (1977) X-Ray analysis of Greek bronze age pigments from Thera (Santorini). Stud Conservat 22:107-115

41. Filippakis SE, Petrakis A, Assimenos K (1979) X-ray analysis of pigments from Vergina (second tomb). Stud Conservat 24:54-58

42. Mirtsou E, Kesisoglou M, Michailidis K (1985) Ανάλυση χρωμάτων και κονιαμάτων μακεδονικού τάφου της περιοχής Λευκαδιών. Ανθρωπολογικά 8: 47-51

43. Linn R (1996) Scientific investigation of the Roman and early Byzantine wall paintings of Caesarea, Israel, Unpublished MA Courtauld Institute of Art, University of London.

44. www.obitel-minsk.by/obitel-minsk_mid496.html

45. Bearat H (1996) Chemical and mineralogical analyses of gallo-roman wall painting from Dietikon, Switzerland. Archaeometry 38:81-95

46. Gillis KM, Robinson PT (1985), Low temperature alteration of the extrusive sequence, Troodos ophiolite, Cyprus, Canadian Mineralogist 23, 431-441

47. Booij E, Gallahan WE, Staudigel H (1995) Ion-exchange experiments and Rb/Sr dating on celadonites from the Troodos ophiolite, Cyprus, Chemical Geology 126, 155-167

48. Segal I, Porat N (1997) Composition of pigments from the Hellenistic walls in Acre. In: Bearat H et al, eds, Roman Wall Painting: Materials, Techniques, Analysis and Conservation: Proceedings of the International Workshop, Fribourg, 7-9 March 1996. pp 85-92

49. Bugini R, Folli L (1997) Materials and Making Techniques of Roman Republican Wall Paintings. In: Bearat H et al, eds, Roman Wall Painting: Materials, Techniques, Analysis and Conservation: Proceedings of the International Workshop, Fribourg, 7-9 March 1996. pp 121–130

50. Brysbaert A (2004) Technology and Social Agency in Bronze Age Aegean and Eastern Mediterranean Painted Plaster. PhD thesis, Department of Archaeology, University of Glasgow, Scotland.

51. Brecoulaki H, Perdikatsis V (2002), Ancient Painting on Macedonian Funerary Monuments,IV-III c B.C: A comparative study on the use of color. In: Tiverios MA, Tsiafakis DS eds, Color in Ancient Greece, pp.147-154, Aristotle University of Thessaloniki

52. Perdikatsis V, Maniatis Y, Saatsoglou-Paliadeli Chr (2002) Characterization of the pigments and the painting technique used on the Vergina stelae. In: Tiverios MA, Tsiafakis DS eds, Color in Ancient Greece, pp.245-258, Aristotle University of Thessaloniki

53. Varone A, Bearat H (1997) Pittori romani al lavoro. Materiali, strumenti, techniche: evidenze archeologiche e dati analitici de un recente scavo pompeiano lungo via dell'Abbondanza (reg. IX ins. 12). In: Roman Wall Painting: Materials, Techniques, Analysis and Conservation: Proceedings of the International Workshop, Fribourg, 7-9 March 1996.

54. Mazzocchin GA, Agnoli F, Mazzocchin S, Colpo I (2003) Analysis of pigments from Roman wall paintings found in Vicenza. Talanta 61:565-572

55. De La Rie E (1982) Fluorescence of paint and varnish layers (Part III). Studies in Conservation. 27, 102-108

56. Wolbers R, Laundrey, G (1987) The use of direct reactive fluorescent dyes for the characterization of binding media in cross sectional examinations. In: AIC Preprints, American Institute for Conservation 15th annual meeting, Vancouver, British Columbia, AIC, Washinghton DC, pp. 168-203

57. Brecoulaki H, Zaitoun C, Stocker SR, Davis JL (2008) An Archer from the Palace of Nestor : A New Wall-Painting Fragment in the Chora Museum, Hesperia 77: 363-97

58. Nevin A, Osticioli I, Anglos D, Burnstock A, Cather S, Castellucci E (2008) The analysis of naturally and artificially-aged protein-based binding media using Raman spectroscopy combined with Principal Component Analysis, J. Raman Spectrosc. 39: 993-1000

59. Cameron MAS, Jones RE, Filippakis SE (1977) Analysis of Fresco Samples form Knossos, Annual British School at Athens 72: pp.123-184

60. Photos-Jones E, Jones RE, Hall AJ (2003) Technical report on painted plaster fragments from the Greek-Swedish excavations at Kastelli, Khania, Crete. Appendix 4. In: Hallager E and Hallager BP, eds, The Greek-Swedish excavations at the Agia Aikaterini Square, Kastelli, Khania, 1970-1987 and 2001: Results of the excavations under the direction of Y Tzedakis and C-G Styrenius, vol III. Astrom Editions, Stockholm, pp 306-320

61. Perdikatsis V (1995) Analysis of pigments from ancient Greek art monuments, in Proc. Scientific Symp. Art and Technology (Athens 1993), Athens, 272-80.

62. Dandrau A (1999) La peinture murale minoenne, I. La palette du peintre égéen et égyptien à l'Age du Bronze. Nouvelles données analytiques. Bulletin de correspondance hellénique 123:1-41

63. Gettens RJ, Duell P (1942) A Review of the problem of Aegean wall painting. Technical Studies, in the Field of the Fine Arts 10:179-223

64. Jones RE, *forthcoming*, Representation in the Aegean: progress towards understanding materials and technology, In J. Bennet, ed. Representation in the Aegean Bronze Age, Sheffield Archaeological Press, Sheffield, UK.

65. Seidel E, Kreuzer H, Harre W (1982) A Late Oligocene/Early Miocene high pressure belt in the External Hellenides, Geol Jb E23: 165-206

LIST OF TABLES

Table 1 Density and mass absorption factors for some minerals that were identified in the plaster samples.

Mineral	Chem. Formula	Density (g/cm^3)	μ (cm^2/g for Cu Ka1)
Calcite	$Ca(CO_3)$	2.7	69.8
Quartz	SiO_2	2.65	33.6
Hematite	Fe_2O_3	5.3	224
Egyptian Blue	$CaCuSi_4O_{10}$	3.1	48.1
Riebeckite	$Na_2Mg_3Fe_2Si_8O_{22}(OH)_2$	3.1	114
Minium	Pb_3O_4	9	209

Table 2 Summary of results of red paint analysis

Sample	LIBS[a]	Raman	XRD	COMMENTS
KN09	Al, Ba, Ca, Fe, Mg, Na, Si, Sr	Hematite	Hematite Calcite Illite Quartz Kaolinite	
KN10	Al, Ba, Ca, Fe, Mg, Na, Si, Sr	Calcite Quartz	X	
KN11	X	Quartz	Quartz	
UM01	Al, Ba, Ca, Fe, Mg, Na, Si, Sr	Hematite	X	
UM04	Al, Ba, Ca, Fe, Mg, Na, Si, Sr	Calcite Gypsum Quartz Fluorescence background	Hematite, Tridymite Calcite	Tridymite is a high temperature polymorph of SiO_2.
UM08	Al, Ba, Ca, Fe, Mg, Na, Si, Sr	Hematite	Hematite Calcite Quartz Kaolinite	
UM10	Al, Ba, Ca, Fe, Mg, Na, Si, Sr	Fluorescence background	-	
UM12	Al, Ba, Ca, Fe, Mg, Na, Si, Sr	Hematite Calcite	-	
VD01	Al, Ba, Ca, Fe, Mg, Na, Pb, Si, Sr, V	Fluorescence background	-	Pb, detected by LIBS , is attributed to lead white
VD02	Al, Ba, Ca, Fe, Mg, Na, Si, Sr	Fluorescence background	-	
VD07	Al, Ba, Ca, Fe, Mg, Na, Si, Sr	Hematite Calcite	-	
VD08	Al, Ba, Ca, Fe, Mg, Na, Si, Sr	Intense fluorescence Egyptian blue	Hematite Quartz	
VD09	-	Hematite	Hematite Calcite Quartz Talc Aragonite	Thin red line not analysed by LIBS
VD10	Al, Ba, Ca, Fe, Mg, Na, Si, Sr	Hematite	Hematite Calcite Quartz,	
VD13	Al, Ba, Ca, Fe, Mg, Na, Si, Sr	Hematite Calcite	-	
VD14	Al, Ba, Ca, Fe, Mg, Na, Si, Sr	Hematite Calcite	-	
G03	Al, Ba, Ca, Fe, Mg, Na, Pb, Si, Sr	Calcite Fluorescence background	Calcite Quartz Illite	Through x-ray mapping, lead seems to be distributed throughout the whole sample
G04	Al, Ba, Ca, Fe, Mg, Na, Si, Sr	Hematite	Hematite Calcite Quartz Kaolinite Glauconite	
G06	Al, Ba, Ca, Fe, Mg, Mn, Pb, Na, Si, Sr	Calcite	Calcite Quartz	Mn, detected by LIBS, is attributed to contamination from black pigment, MnO_2
G10	Al, Ba, Ca, Fe, Mg, Mn, Na, Si, Sr	Hematite Calcite	Calcite Quartz Kaolinite	Mn, detected by LIBS, is attributed to contamination from black pigment, MnO_2

a Underlined element indicates correlation with the main pigment mineral

Table 3 Summary of results of yellow paint analysis

Sample	LIBS[a]	Raman	XRD	Comments
KN08	Al, Ba, Ca, Fe, Mg, Na, Si, Sr	-	Hematite	
UM07	Al, Ba, Ca, Fe, Mg, Na, Si, Sr	Goethite	-	
UM10	Al, Ba, Ca, Fe, Mg, Na, Si, Sr	Goethite	-	
UM12	Al, Ba, Ca, Fe, Mg, Na, Si, Sr	-	-	
VD09	Al, Ba, Ca, Fe, Mg, Na, Si, Sr	Goethite Calcite	Hematite	
VD10	Al, Ba, Ca, Fe, Mg, Na, Si, Sr	Goethite	Goethite	
G10	Al, Ba, Ca, Fe, Mg, Na, Si, Sr, Zn	-	Kaolinite	

a Underlined element indicates correlation with the main pigment mineral

Table 4 Summary of results of blue paint analysis

Sample	LIBS[a]	Raman	XRD	SEM-EDX (X-ray mapping)	Comment
KN01	see Table 6	see Table 6	Calcite Talc Riebeckite Muscovite, Quartz Clinochlore	Calcite Talc Mg-Riebeckite Muscovite Quartz Clinochlore	Macroscopically the color is black but in polish section Grey-blue
KN02	Al, Ba, Ca, Fe, Mg, Na, Si, Sr	Intense fluorescence at 890 nm Egyptian Blue	Riebeckite Calcite Talc Muscovite, Quartz	Mg-Riebeckite Calcite Talc Muscovite Quartz	~ 30-80µm red layer over a ~200µm layer of Mg-Riebeckite and Egyptian Blue (see Fig. 2)
KN03	Al, Ba, Ca, Cu, Fe, Mg, Na, Si, Sr	Intense fluorescence at 890 nm Egyptian Blue	Cuprorivaite Calcit Quartz Kaolinite	-	
KN04	Al, Ba, Ca, Cu, Fe, Mg, Na, Si, Sr	Intense fluorescence at 890 nm Egyptian Blue	Cuprorivaite Calcite Cuprite Talc Riebeckite Illite	-	
KN05	Al, Ba, Ca, Cu, Fe, Mg, Na, Si, Sr	Intense fluorescence at 890 nm Egyptian Blue	Cuprorivaite Calcite	-	
KN06	Al, Ba, Ca, Cu, Fe, Mg, Na, Si, Sr	Intense fluorescence at 890 nm Egyptian Blue	Cuprorivaite Calcite Talc Riebeckite Muscovite Chlorite	Cuprorivaite, CalciteTalc Mg-Riebeckite Muscovite Chlorite	~200µm layer similar to KN01
KN11	Al, Ba, Ca, Fe, Mg, Na, Si, Sr	-	Cuprorivaite Calcite Illite Quartz Paragonite	-	
UM01	Al, Ba, Ca, Fe, Mg, Na, Si, Sr	-	Cuprorivaite Calcite Quartz	-	
UM06	Al, Ba, Ca, Cu, Fe, Mg, Na, Si, Sr	Intense fluorescence at 890 nm Egyptian Blue	-	-	
UM12	Al, Ba, Ca, Cu, Fe, Mg, Na, Si, Sr	Intense fluorescence at 890 nm Egyptian Blue	-	-	
VD01	Al, Ba, Ca, Cu, Fe, Mg, Na, Pb, Si, Sr	Intense fluorescence at 890 nm Egyptian Blue	-	-	
VD04	Al, Ba, Ca, Cu, Fe, Mg, Na, Pb, Si, Sr	Intense fluorescence at 890 nm Egyptian Blue	Cuprorivaite Calcite Quartz Cristobalite	-	Cristobalite is relict or residue from the Egyptian Blue synthesis
VD08	Al, Ba, Ca, Cu, Fe, Mg, Na, Si, Sr	Intense fluorescence at 890 nm Egyptian Blue	Cuprorivaite Calcite Quartz Hematite		

			Dioptase		
VD09	Al, Ba, Ca, Cu, Fe, Mg, Na, Si, Sr	Intense fluorescence at 890 nm Egyptian Blue	Calcite Quartz Hematite Talc Aragonite	-	
G01	Al, Ba, Ca, Cu, Fe, Mg, Na, Pb, Si, Sr	Calcite	-	-	
G04	Al, Ba, Ca, Fe, Mg, Na, Si, Sr	-	Calcite Quartz Kaolinite Hematite Glauconite	-	
G06	Al, Ba, Ca, Cu, Fe, Mg, Na, Si, Sr	-	Calcite Quartz	-	
G07	Al, Ba, Ca, Fe, Mg, Na, Si, Sr	Calcite	Calcite Quartz	-	
G10	Al, Ba, Ca, Fe, Mg, Si, Sr, Zn	-	Calcite Quart Kaolinite	-	
G11	Al, Ba, Ca, Cu, Fe, Mg, Na, Si, Sr	Phthaloc. blue Calcite	Calcite Quartz Hematite Chlorite	-	
G12	Al, Ba, Ca, Cu, Fe, Mg, Na, Si, Sr	Phthaloc. blue Calcite	Calcite Quartz,	-	

a Underlined element indicates correlation with the main pigment mineral

Table 5 Summary of results of green paint analysis

Sample	LIBS[a]	Raman	XRD	COMMENTS
UM01	Al, Ba, Ca, Fe, Mg, Na, Si, Sr	Intense fluorescence at 890 nm Egyptian Blue	Calcite Quartz Cuprorivaite	
UM02	Al, Ba, Ca, Fe, Mg, Na, Si, Sr	Intense fluorescence at 890 nm Egyptian Blue	-	
UM09	Al, Ba, Ca, Fe, Mg, Na, Si, Sr	Weak fluorescence at 890 nm Egyptian Blue	-	See Table 6
UM11	Al, Ba, Ca, Fe, Mg, Na, Si, Sr	No Raman bands	-	
VD02	Al, Ba, Ca, Fe, Mg, Na, Si, Sr	No Raman bands	-	
VD03	Al, Ba, Ca, Fe, Mg, Na, Si, Sr	No Raman bands	-	
VD05	Al, Ba, Ca, Fe, Mg, Na, Si, Sr	No Raman bands	-	
VD06	Al, Ba, Ca, Fe, Mg, Na, Si, Sr	Calcite	Calcite Quartz Hematite	
VD08	Al, Ba, Ca, Cu, Fe, Mg, Na, Si, Sr	Intense fluorescence at 890 nm Egyptian Blue	-	
VD09	Al, Ba, Fe, Ca, Mg, Na, Si, Sr	Intense fluorescence at 890 nm Egyptian Blue	-	
VD12	Al, Ba, Ca, Fe, Mg, Na, Si, Sr	No Raman bands	-	
G02	Al, Ba, Ca, Fe, Mg, Na, Si, Sr	No Raman bands	Calcite Quartz	
G05	Al, Ba, Ca, Fe, Mg, Na, Si, Sr	-	-	
G07	Al, Ba, Ca, Fe, Mg, Na, Si, Sr	-	Calcite Quartz	
G08	Al, Ba, Ca, Cr, Fe, Mg, Na, Si, Sr	-	Calcite Quartz Celadonite Chlorite	Al, Ca, Cr, Fe, Mg, K, Si observed in SEM-EDX; chromite is detected through X-ray mapping
G09	Al, Ba, Ca, Fe, Mg, Na, Si, Sr	No Raman bands	Quartz Calcite Cuprorivaite Chlorite	

a Underlined element indicates correlation with the main pigment mineral

Table 6 Summary of results of black and grey paint analysis

Sample	LIBS[a]	Raman	XRD	COMMENTS
KN01	Al, Ba, Ca, Fe, Mg, Na, Si, Sr	No Raman bands	Calcite Talc Riebeckite, Muscovite Quartz Clinochlore	Raman analysis with excitation at 473nm shows graphite bands(carbon black)
KN02	Al, Ba, Ca, Fe, Mg, Na, Si, Sr	-	Calcite Talc Riebeckite Muscovite Quartz	
KN06 / grey	-	Intense fluoresence at 890 nm Egyptian blue	Calcite Talc Cuprorivaite Riebeckite Muscovite Chlorite	
KN07	Al, Ba, Ca, Fe, Mg, Na, Si, Sr	No Raman bands	Calcite Cuprorivaite Illite Quartz	
UM02	Al, Ba, Ca, Fe, Mg, Na, Si, Sr	-	-	
UM03	Al, Ba, Ca, Fe, Mg, Na, Si, Sr	No Raman bands	Calcite Quartz Cuprorivaite	
UM05	Al, Ba, Ca, Fe, Mg, Na, Si, Sr	No Raman bands	Calcite Quartz Fluorapatite	Quartz crystals were aslo identified through X-ray mapping of polished cross section (Fig. 16)
UM09	Al, Ba, Ca, Fe, Cu, Mg, Na, Si, Sr	No Raman bands	-	Raman analysis with excitation at 473nm shows graphite bands(carbon black) when laser is focused on very dark coloured particles
UM10 / grey	Al, Ba, Ca, Fe, Cu, Mg, Na, Si, Sr	Intense fluoresence at 890 nm Egyptian blue	Calcite Quartz Cuprorivaite	
UM12 / grey	-	Calcite	-	
VD01	Al, Ba, Ca, Cu, Fe, Mg, Na, Pb, Si, Sr	-	-	
VD05	Al, Ba, Ca, Fe, Mg, Na, Si, Sr	-	-	
VD06	Al, Ba, Ca, Fe, Mg, Na, Si, Sr	No Raman bands	-	
VD11	Al, Ba, Ca, Fe, Mg, Na, Si, Sr	-	-	
G01 / black	Al, Ba, Ca, Cu, Fe, Mg, Mn, Na, Pb, Si, Sr	No Raman bands	-	
G05	Al, Ba, Ca, Fe, Mg, Na, Si, Sr	Calcite	-	

a Underlined element indicates correlation with the main pigment mineral

FIGURE CAPTIONS

Fig. 1 Diagram of the calculated penetration depth values of Cu Kα x-ray radiation for minerals identified in the plaster samples, as a function of 2θ.

Fig. 2 Polished cross-section of paint sample taken from wall painting KN02. Total paint thickness, d, is approximately 280 μm. A thin red layer overlays a thicker blue one. Several blue pigment grains are clearly visible, and have been identified by SEM-EDX analysis and X-ray mapping as Egyptian blue (1, 3) and Mg-Riebeckite (2, 4). See also Fig. 13.

Fig. 3 LIBS spectrum of red painted plaster, G04. (Note: the broad bands in the range of 550-570 nm and 600-650 nm are attributed to emission from excited CaO formed in the laser ablation plume). Inset: Detailed view of the spectrum in the range of 410-450 nm where distinct Fe and Ca emission lines are observed.

Fig. 4 Mean value of the raw intensity (not normalized) of the Fe emission line at 438.354 nm for the different paints analysed in all the wall painting fragments investigated. LIBS spectra corresponding to the second laser pulse irradiating the paint have been used in order to minimize the influence of surface impurities affecting spectra obtained with the first pulse.

Fig. 5 Detail of LIBS spectrum obtained from the red painted area of plaster fragment VD01. Pb emission lines : 357.273, 363.957, 368.346, 373.994, 405.78 nm.

Fig. 6 Raman spectra obtained from red painted plasters and a sample of pure hematite (The band at 370 cm^{-1} has been confirmed to have its origin on an instrumental artefact).

Fig. 7 Raman spectra from red plasters UM04 and G06 showing bands from calcite and calcite gypsum and quartz respectively but no bands from hematite or lead white. The UM04 spectrum has not been baseline corrected in order to show the intense broadband background fluorescence.

Fig. 8 Raman spectra from yellow painted plaster fragments VD10. The spectrum of pure yellow ochre is shown for comparison**.**

Fig. 9 Cu emission lines (324.754 nm and 327.396 nm) in the LIBS spectrum obtained from blue paint on VD04.

Fig. 10 LIBS depth profiling of red over blue paint in sample VD08.

Fig. 11 Fluorescence emission spectrum collected on the Raman spectrometer from two areas on sample UM 02 (blue grain: solid line; green particles; dashed line).

Fig. 12 X-Ray diffractograms of samples KN04 (a) and VD08 (b). Mineral phases identified are indicated by numbers. 1: Calcite ($CaCO_3$); 2: Cuprorivaite (Egyptian blue, $CaCuSi_4O_{10}$); 3: Quartz (SiO_2); 4: Talc ($Mg_3(OH)_2Si_4O_{10}$); 5: Mg-Riebeckite ($Na_{1.38}K_{0.13}Ca_{0.17}Mg_{0.25}Mg_{2.81}Fe_{1.66}Fe_{0.48}Al_{0.04}Si_{7.94}O_{22}(OH)_2$); 6: Muscovaite ($KAl_3Si_3O_{10}(OH)_2$); 7: Hematite (alpha-Fe_2O_3); 8: Dioptase ($CuSiO_2(OH)_2$).

Fig.13 SEM images with elemental analysis mapping for samples KN02 (top) and KN06 (bottom). Mineral particles marked correspond to Mg-Riebeckite / Si, Fe, Mg, Al (1); Egyptian blue / Si, Ca, Cu (2); Quartz / Si (3) and Calcite (4).

Fig. 14 SEM image with elemental analysis mapping from sample G08. Mineral particles marked correspond to Chromite / Cr, Fe (1); Celadonite / Ca, Si, K, Fe, Mg, Al (2); Quartz / Si (3).

Fig. 15 Part of LIBS spectrum collected on black painted plaster, G01, showing the presence of Mn. Emission lines (470.972, 472.748, 473.911, 475.404, 476.153/476.238, 476.586/476.643, 478.342, 482.352 nm).

Fig. 16 SEM image with elemental analysis mapping from sample UM05. Mineral particles marked correspond to Quartz / Si (1).

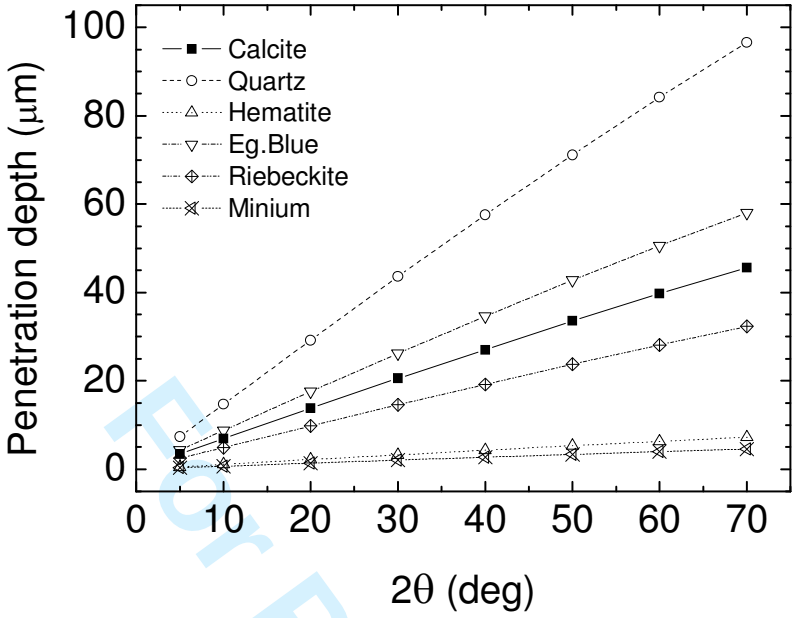

Fig. 1

Fig. 1 Diagram of the calculated penetration depth values of Cu Kα x-ray radiation, for, minerals identified in the plaster samples, as a function of 2θ.

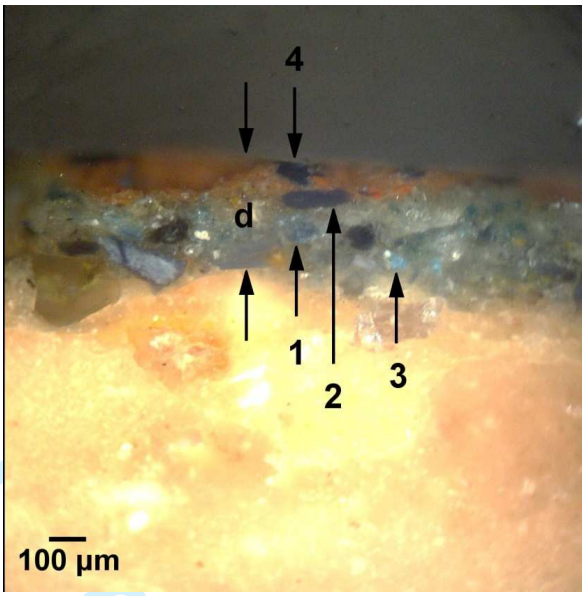

Fig. 2

Fig. 2 Polished cross-section of paint sample taken from wall painting KN02. Total paint thickness, d, is approximately 280 µm. A thin red layer overlays a thicker blue one. Several blue pigment grains are clearly visible, and have been identified by SEM-EDX analysis and X-ray mapping as Egyptian blue (1, 3) and Mg-Riebeckite (2, 4). See also Fig. 13.

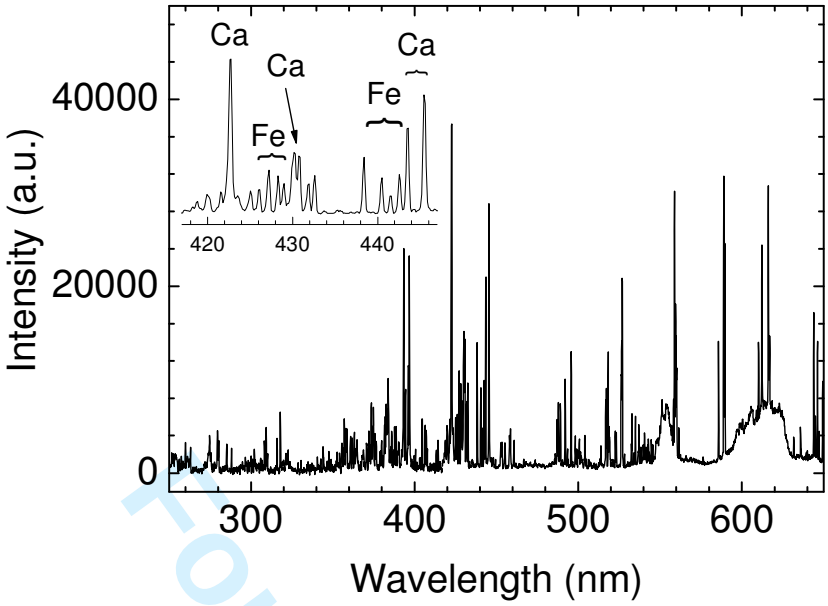

Fig. 3

Fig. 3 LIBS spectrum of red painted plaster, G04. (Note: the broad bands in the range of 550-570 nm and 600-650 nm are attributed to emission from excited CaO formed in the laser ablation plume). Inset: Detailed view of the spectrum in the range of 410-450 nm where distinct Fe and Ca emission lines are observed.

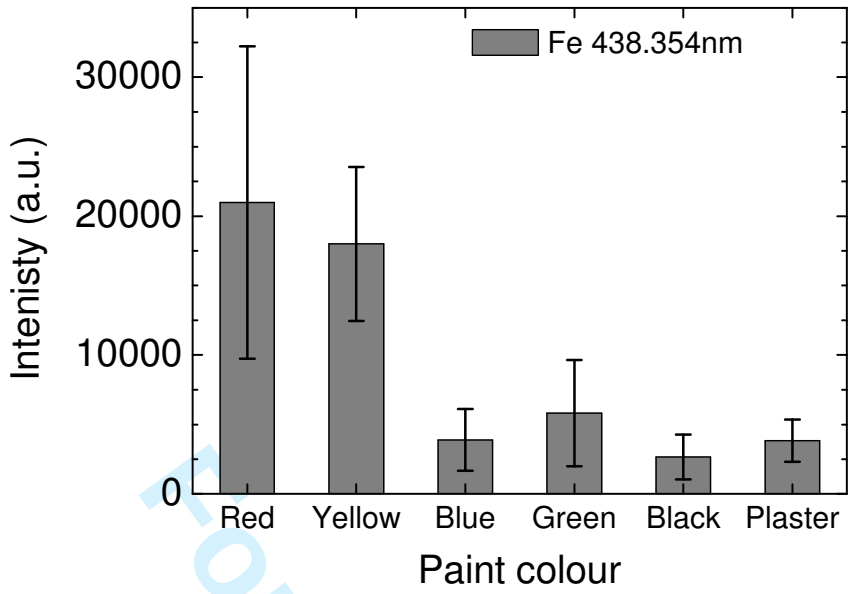

Fig. 4

Fig. 4 Mean value of the raw intensity (not normalized) of the Fe emission line at 438.354 nm for the different paints analysed in all the wall painting fragments investigated. LIBS spectra corresponding to the second laser pulse irradiating the paint have been used in order to minimize the influence of surface impurities affecting spectra obtained with the first pulse.

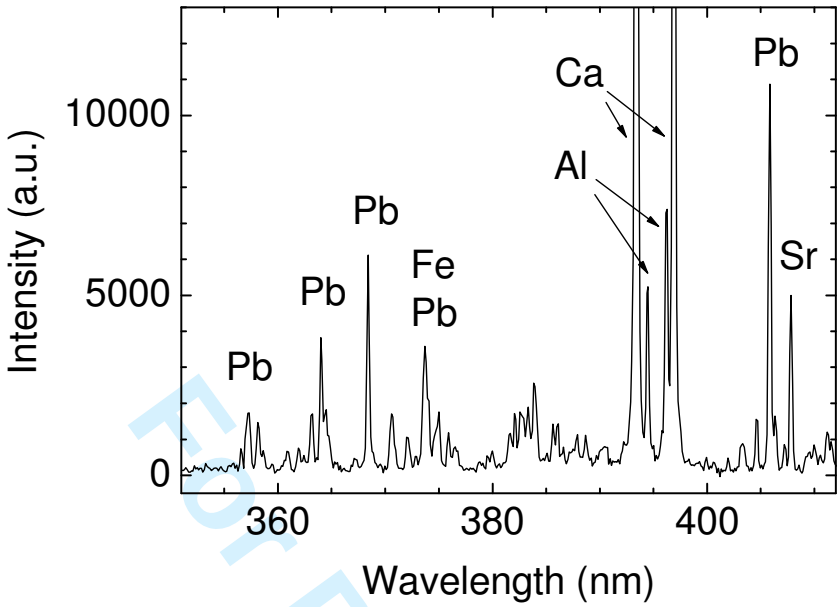

Fig. 5

Fig. 5 Detail of LIBS spectrum obtained from the red painted area of plaster fragment VD01.

Pb emission lines : 357.273, 363.957, 368.346, 373.994, 405.78 nm.

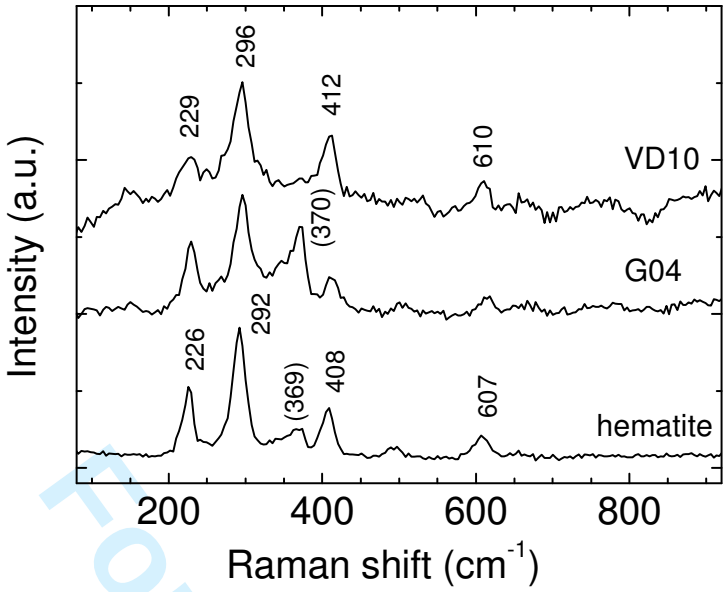

Fig. 6

Fig. 6 Raman spectra obtained from red painted plasters and a sample of pure hematite (The band at 370 cm^{-1} has been confirmed to have its origin on an instrumental artefact).

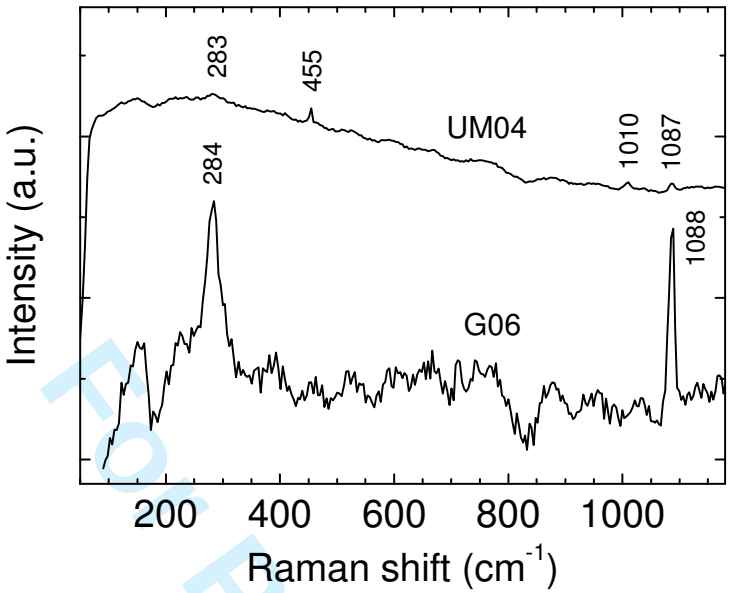

Fig. 7

Fig. 7 Raman spectra from red plasters UM04 and G06 showing bands from calcite and calcite gypsum and quartz respectively but no bands from hematite or lead white. The UM04 spectrum has not been baseline corrected in order to show the intense broadband background fluorescence.

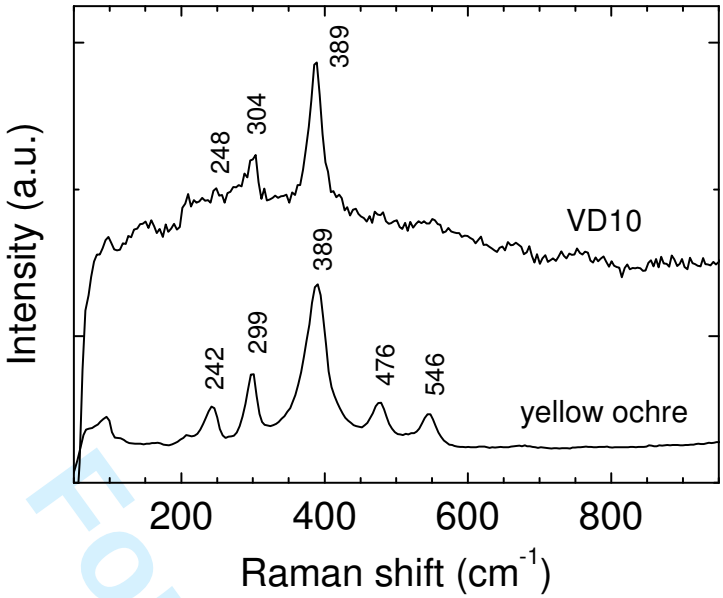

Fig. 8

Fig. 8 Raman spectra from yellow painted plaster fragments VD10. The spectrum of pure yellow ochre is shown for comparison**.**

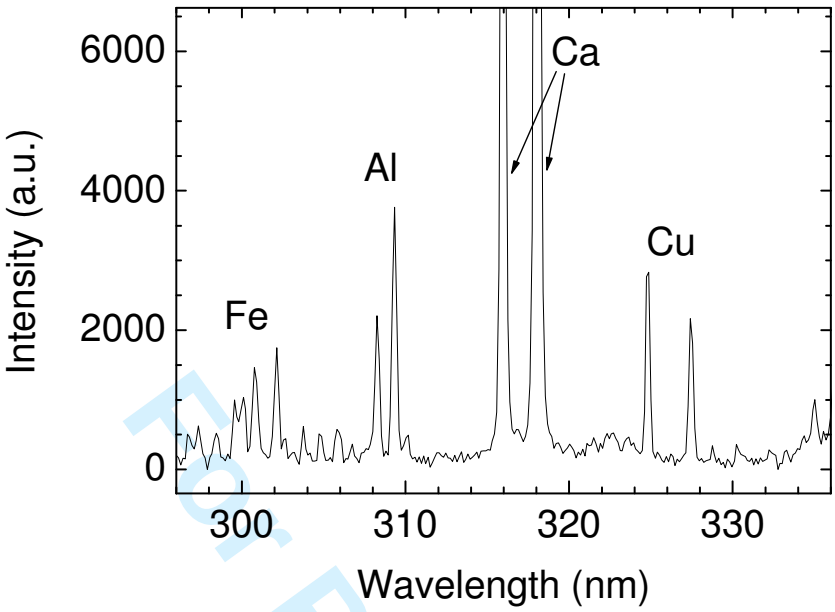

Fig. 9

Fig. 9 Cu emission lines (324.754 nm and 327.396 nm) in the LIBS spectrum obtained from blue paint on VD 04 blue pigment.

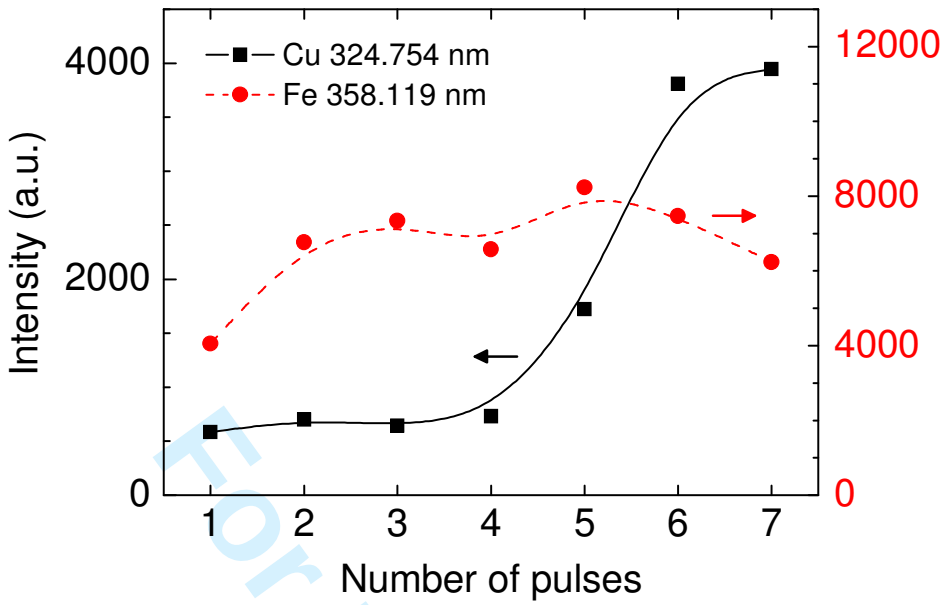

Fig. 10

Fig. 10 LIBS depth profiling of red over blue paint in sample VD08.

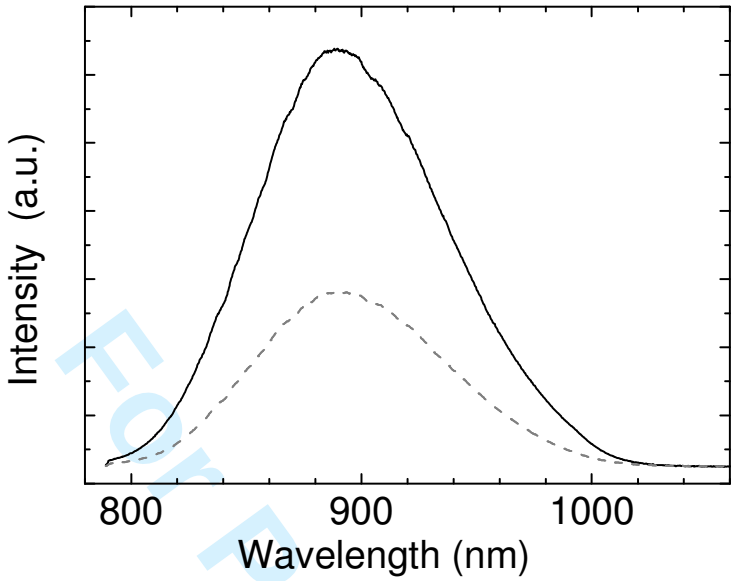

Fig. 11

Fig. 11 Fluorescence emission spectrum collected on the Raman spectrometer from two areas on sample UM 02 (blue grain: solid line; green particles; dashed line).

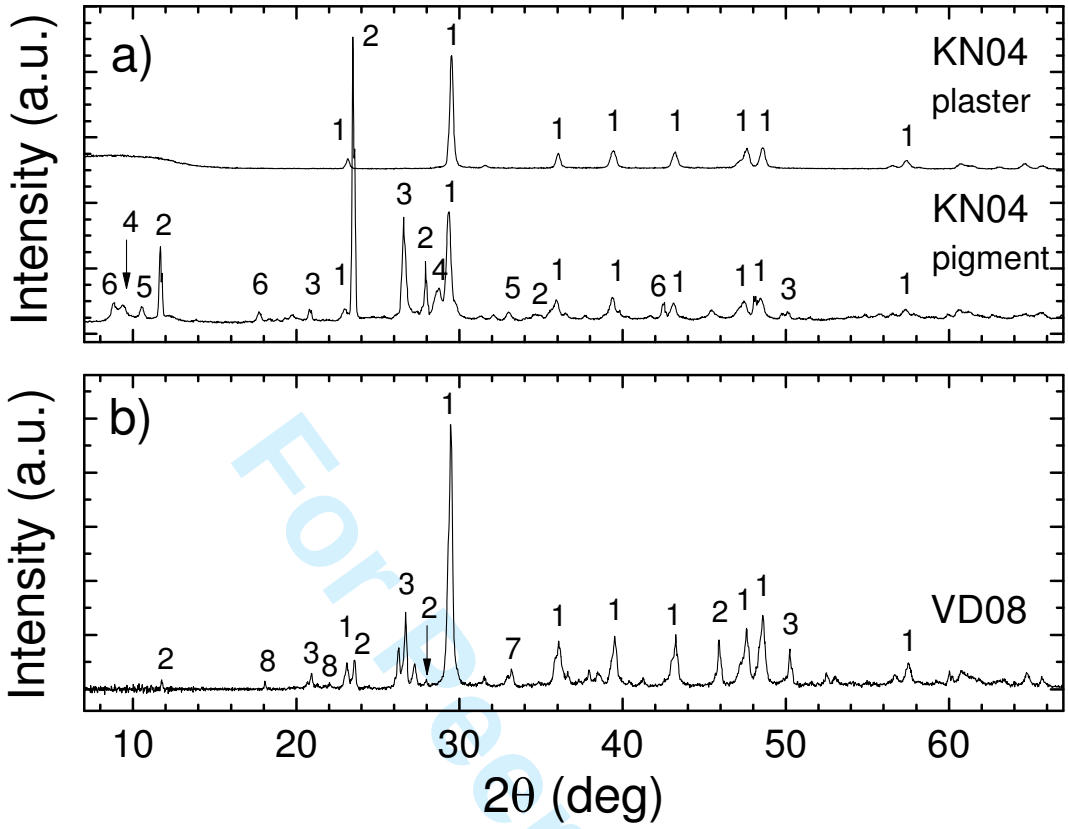

Fig. 12

Fig. 12 X-Ray diffractograms of samples KN04 (a) and VD08 (b). Mineral phases identified are indicated by numbers. 1: Calcite ($CaCO_3$); 2: Cuprorivaite (Egyptian blue, $CaCuSi_4O_{10}$); 3: Quartz (SiO_2); 4: Talc ($Mg_3(OH)_2Si_4O_{10}$); 5: Mg-Riebeckite ($Na_{1.38}K_{0.13}Ca_{0.17}Mg_{0.25}Mg_{2.81}Fe_{1.66}Fe_{0.48}Al_{0.04}Si_{7.94}O_{22}(OH)_2$); 6: Muscovaite ($KAl_3Si_3O_{10}(OH)_2$); 7: Hematite (alpha-Fe_2O_3); 8: Dioptase ($CuSiO_2(OH)_2$).

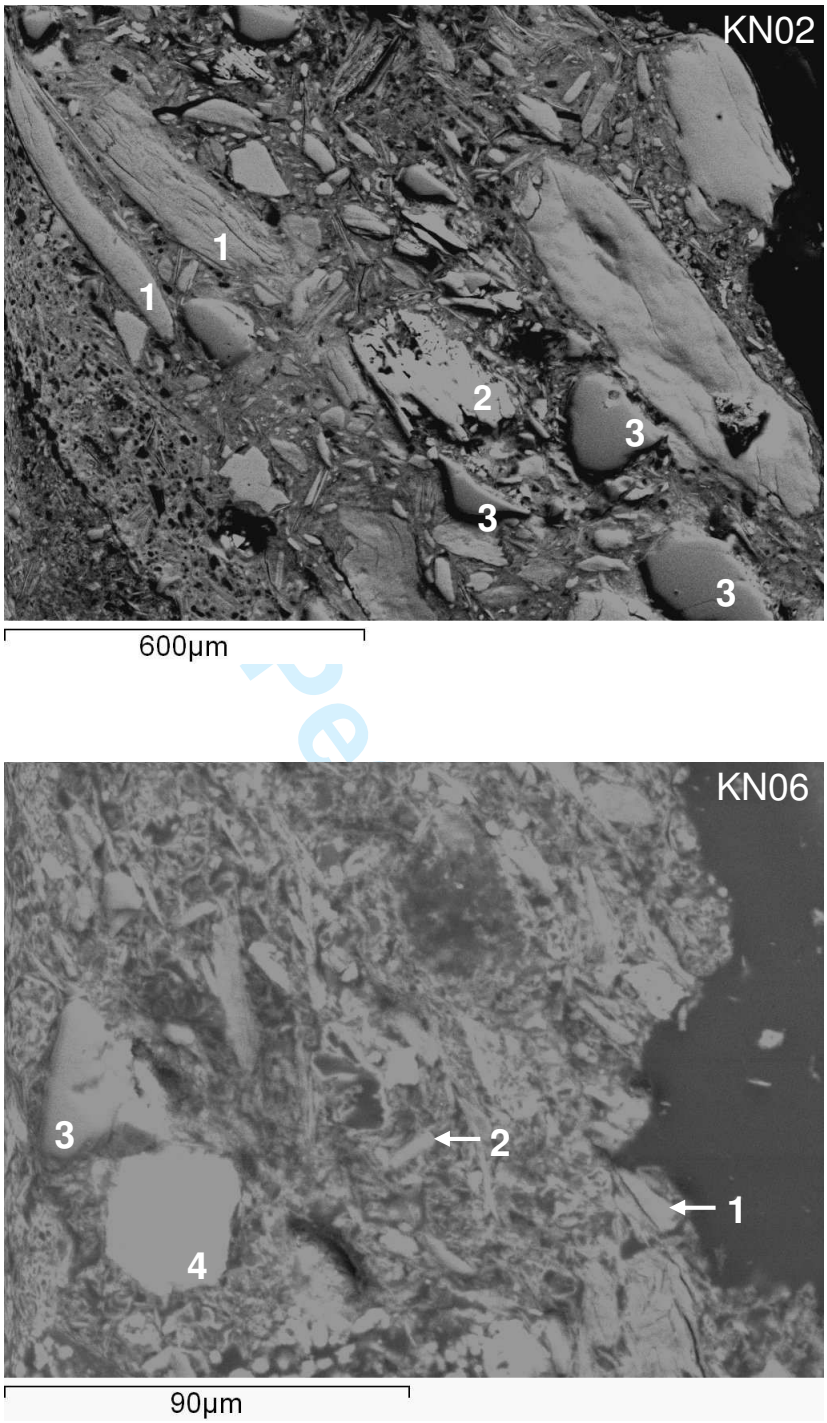

Fig. 13

Fig.13 SEM images with elemental analysis mapping for samples KN02 (top) and KN06 (bottom). Mineral particles marked correspond to Mg-Riebeckite / Si, Fe, Mg, Al (1); Egyptian blue / Si, Ca, Cu (2); Quartz / Si (3) and Calcite (4).

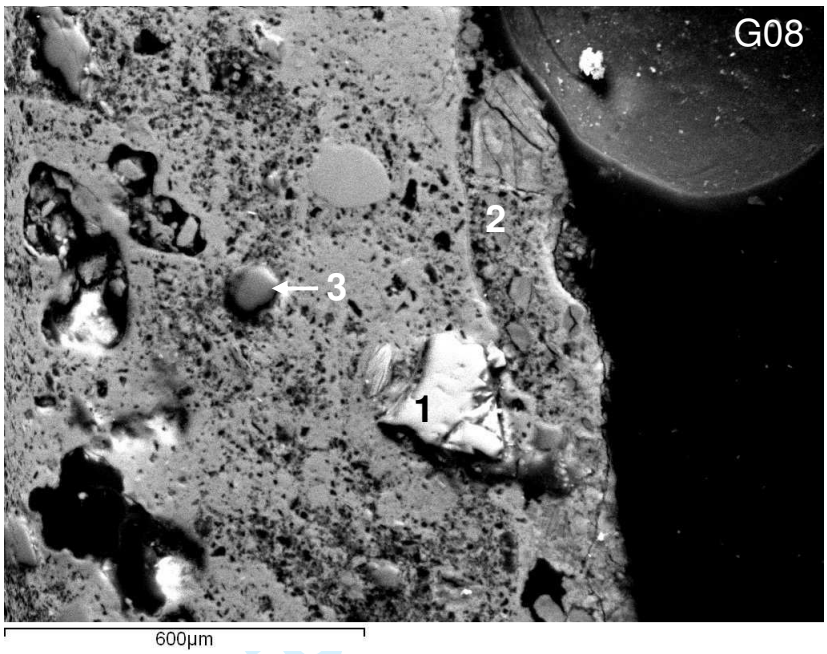

Fig. 14

Fig. 14 SEM image with elemental analysis mapping from sample G08. Mineral particles marked correspond to Chromite / Cr, Fe (1); Celadonite / Ca, Si, K, Fe, Mg, Al (2); Quartz / Si (3).

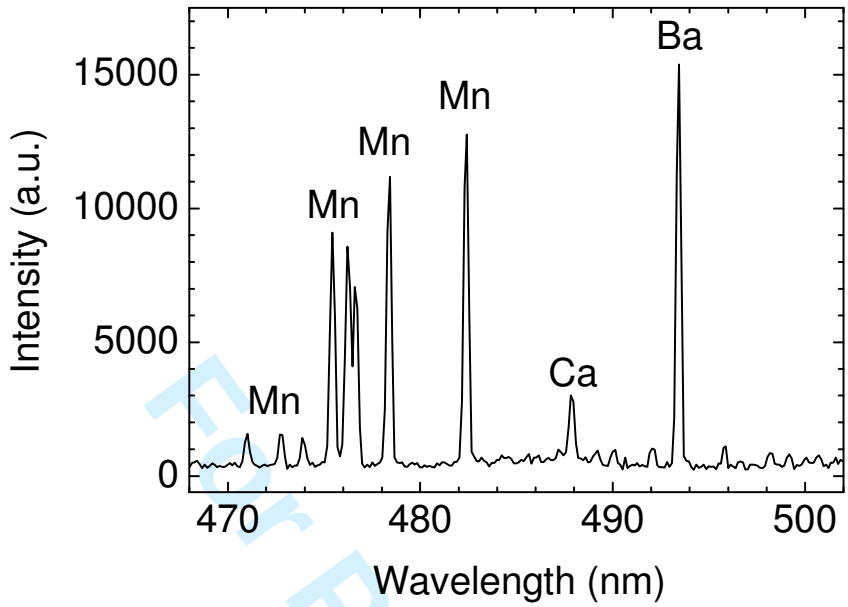

Fig. 15

Fig. 15 Part of LIBS spectrum collected on black painted plaster, G01, showing the presence of Mn. Emission lines (470.972, 472.748, 473.911, 475.404, 476.153/476.238, 476.586/476.643, 478.342, 482.352 nm).

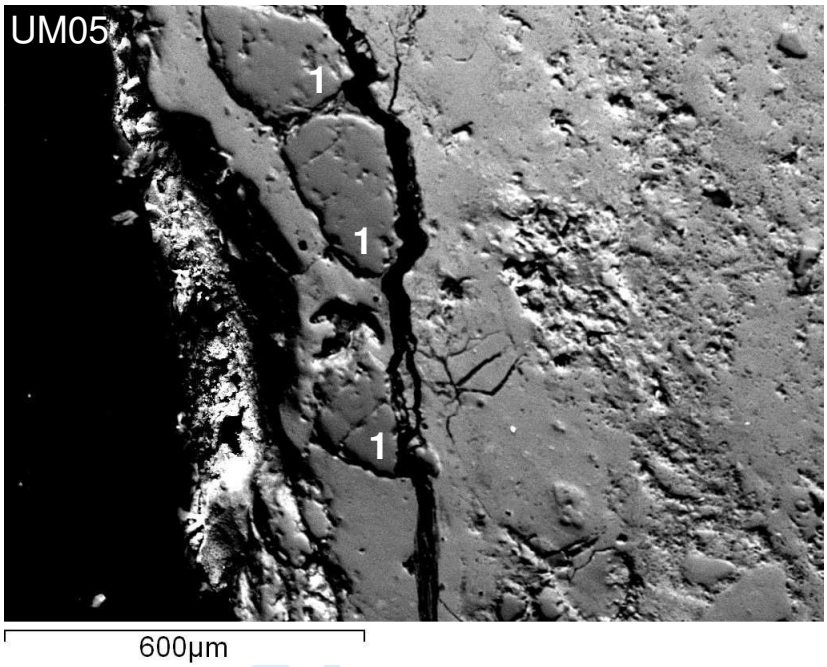

Fig. 17

Fig. 16 SEM image with elemental analysis mapping from sample UM05. Mineral particles marked correspond to Quartz / Si (1).

Analytical and Bioanalytical Chemistry

Electronic Supplementary Material

Studying pigments on painted plaster in Minoan, Roman and Early Byzantine Crete. A multi-analytical technique approach

P. Westlake, P. Siozos, A. Philippidis, C. Apostolaki, B. Derham, A. Terlixi, V. Perdikatsis, R. Jones, D. Anglos

Fig. S1 Raman spectrum of blue paint on wall painting G11. Peaks marked by asterisk are attributed to phthalocyanine blue.

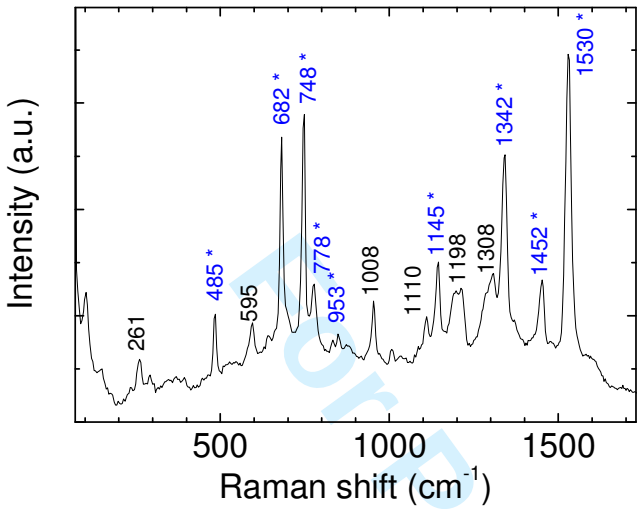

Fig. S2 Distribution of the blue minerals glaucophane and crossite/riebeckite within the phyllite-quartzite unit in Crete; the former is more common in the west of the island, the latter in the east. (Adapted from Ref. 65, Fig. 8).

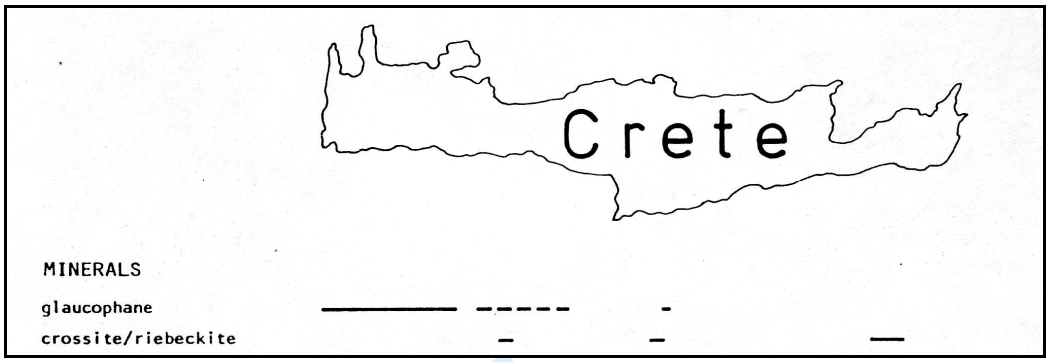

Analytical and Bioanalytical Chemistry

Electronic Supplementary Material

Studying pigments on painted plaster in Minoan, Roman and Early Byzantine Crete. A multi-analytical technique approach

P. Westlake, P. Siozos, A. Philippidis, C. Apostolaki, B. Derham, A. Terlixi, V. Perdikatsis, R. Jones, D. Anglos

Fig. S1 Raman spectrum of blue paint on wall painting G11. Peaks marked by asterisk are attributed to phthalocyanine blue.

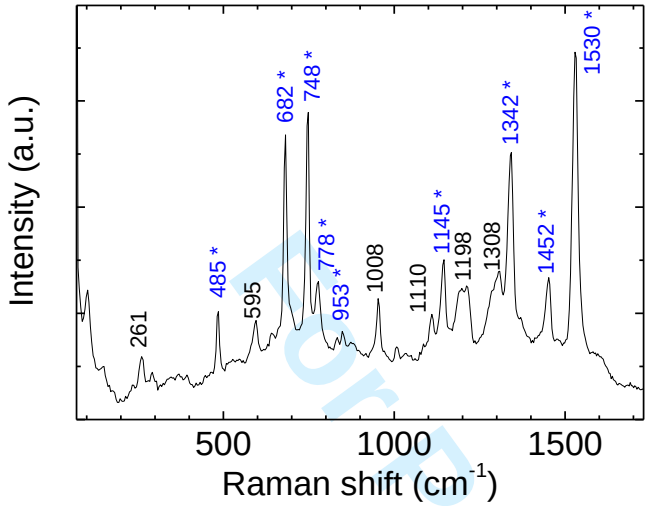

Fig. S2 Distribution of the blue minerals glaucophane and crossite/riebeckite within the phyllite-quartzite unit in Crete; the former is more common in the west of the island, the latter in the east. (Adapted from Ref. 65, Fig. 8).